European Journal of Medicinal Chemistry 303 (2026) 118445

Contents lists available at ScienceDirect

European Journal of Medicinal Chemistry

journal homepage: www.elsevier.com/locate/ejmech

Research paper

N-Acylaminoethyltetrahydroquinolines: A new class of melatonin receptor ligands with in vivo activity on glioblastoma

Annalida Bedini [a], Francesca Galvani [b,1], Gian Marco Elisi [a], Laura Scalvini [b], Michele Mari [a], Adriano Recchia [a], Pedro Augusto C.M. Fernandes [c], Gabriela S. Kinker [d], Valeria Lucini [e], Francesco Scaglione [e], Fabrizio Vincenzi [f], Katia Varani [f], Regina P. Markus [c], Silvia Rivara [b,*], Gilberto Spadoni [a], Marco Mor [b]

[a] *Dipartimento di Scienze Biomolecolari, Università degli Studi di Urbino Carlo Bo, Piazza Rinascimento 6, 61029, Urbino, Italy*
[b] *Dipartimento di Scienze degli Alimenti e del Farmaco, Università degli Studi di Parma, Parco Area delle Scienze 27/A, 43124, Parma, Italy*
[c] *Department of Physiology, Institute of Bioscience, University of São Paulo, São Paulo, Brazil*
[d] *International Research Center, A. C. Camargo Cancer Center, São Paulo, Brazil*
[e] *Dipartimento di Oncologia ed Emato-Oncologia, Università degli Studi di Milano, Via Vanvitelli 32, 20129, Milano, Italy*
[f] *Dipartimento di Medicina Traslazionale, Università degli Studi di Ferrara, Ferrara, Italy*

ARTICLE INFO

Keywords:
Glioblastoma
Melatonin
Subtype-selective receptor modulator
Molecular modelling
Structure-activity relationships

ABSTRACT

Tetrahydroquinoline (THQ) derivatives bearing an N-acylaminoethyl side chain were investigated as a new class of potent melatonergic ligands offering opportunities for a versatile modulation of binding and pharmacological properties. These compounds were designed from N-anilinoethylamide ligands by formal closure of the N-substituent into an additional fused ring. Molecular modelling studies, including alchemical simulations, allowed to rationalize configurational and conformational aspects of ligand activity and supported the role of the THQ nucleus in the MT_2 receptor selectivity observed for these compounds when compared to N-anilinoethylamide counterparts. The moderate stereoselectivity generated by substituents in position 2 of the THQ ring or at the β-position of the ethylamide chain could be ascribed to the conformational enrichment of ligand poses fitting the receptor binding site observed for the eutomer.

Replacement of the methoxy group with bulkier substituents was investigated to differentially modulate intrinsic activity at the MT_1 and MT_2 receptor subtypes. Mixed activity, with MT_1 agonist and MT_2 antagonist profile, could be achieved by insertion of a 7-(2-hydroxyethoxy) group, as already observed for compound 5-HEAT. UCM1400 (**4d**) was more potent than 5-HEAT and emerged as a promising pharmacological tool for targeting glioblastoma. The compound exhibited in vitro antiproliferative activity on human glioma cell lines and was effective in vivo, reducing tumor growth in a U87MG orthotopic xenograft mouse model. These findings support the development of subtype-selective modulators of melatonin receptors as a promising new avenue for cancer therapy.

1. Introduction

The neurohormone melatonin (**1**, *N*-acetyl-5-methoxytryptamine, Fig. 1) is primarily synthesized by the pineal gland following a circadian rhythm, with peak production and release in the plasma and cerebrospinal fluid during the dark phase when the inhibitory effect exerted by light is not present. Melatonin produced in other organs and tissues, such as the retina according to a circadian rhythm, or the skin, gut and bone marrow in a noncircadian manner, essentially acts locally, with paracrine or autocrine effects. Melatonin exerts most of its

Abbreviations: DCAD, *p*-chlorobenzyl-azodicarboxylate; DCM, dichloromethane; DIAD, diisopropyl azodicarboxylate; DMF, dimethylformamide; ECL, extracellular loop; FES, free energy surface; IL, intracellular loop; MsCl, mesyl chloride; PBS, Phosphate-buffered saline; TES, triethylsilane; TFA, trifluoroacetic acid; THQ, tetrahydroquinoline; TI, thermodynamic integration; TCEP, tris(2-carboxyethyl)phosphine.

* Corresponding author. Dipartimento di Scienze degli Alimenti e del Farmaco, Parco Area delle Scienze 27/A, 43124 Parma, Italy.
E-mail address: silvia.rivara@unipr.it (S. Rivara).
[1] Present address: Department of Anatomy and Neurobiology, University of California, Irvine, Irvine, CA, USA.

https://doi.org/10.1016/j.ejmech.2025.118445
Received 11 August 2025; Received in revised form 21 November 2025; Accepted 29 November 2025
Available online 3 December 2025
0223-5234/© 2025 The Authors. Published by Elsevier Masson SAS. This is an open access article under the CC BY license (http://creativecommons.org/licenses/by/4.0/).

activities through the activation of MT_1 and MT_2 G protein-coupled receptors (GPCRs) [1,2]. MT_1 and MT_2 receptors mainly couple to G_i protein, reducing cAMP levels, even if other signaling systems have been identified for both receptors. The activity of melatonin receptors is also regulated by their ability to homo- and heterodimerize between each other and with other GPCRs, further modulating intracellular signaling activity and functional properties, by the presynaptic localization affecting neurotransmitter release [3,4], and by possible biased signaling of synthetic ligands [5]. Melatonin receptors signal photoperiodic information and control daily rhythms, such as the sleep-wake cycle, which makes melatonin a widely used dietary supplement to alleviate the symptoms of jet-lag. Controlled-release formulations of melatonin are also prescribed for the treatment of insomnia. Besides these and other central nervous system-related activities, melatonin modulates the physiological functions of several peripheral systems and organs, such as the immune and cardiovascular systems, affects glucose and lipid homeostasis and has been proposed for the prevention and treatment of diverse conditions, spanning from neurodegenerative diseases to cancer [3,6].

In the last decades, several melatonin receptor ligands have been described and the MT_1/MT_2 nonselective agonists ramelteon, agomelatine and tasimelteon have reached the market to treat insomnia, depression and non-24-h sleep-wake disorder in blind individuals, respectively. Additionally, melatonin receptor ligands with different pharmacological profiles were also synthesized and MT_1-or MT_2-subtype selective compounds have been obtained, as well as ligands with partial agonist, antagonist or inverse agonist activity [7–9]. These pharmacological tools, coupled with the identification of receptor distribution and the availability of MT_1/MT_2 knockout animals have allowed the characterization of the role of the two receptor subtypes. Even if we are still far from a complete understanding of the peculiarities and differences between MT_1 and MT_2, it is clear that they do not share the same tissue distribution [10] and mediate different activities, both in physiological contexts and in disease conditions. The MT_1 receptor has been described to be able to inhibit neuronal firing in mouse hypothalamic suprachiasmatic nucleus and prolactin secretion in photoperiodic species, to regulate rapid eye movement sleep [11] and enhance body temperature [12]. Vasoconstriction in rat caudal artery [13], modulation of visual function, and lymphocyte differentiation are also mediated by MT_1 receptor activation. The MT_2 receptor produces phase-shifting of circadian rhythms in the hypothalamic suprachiasmatic nucleus and promotes non-REM sleep in rodents [14] and rat caudal artery vasodilation. In some cases, as observed in brain tumor progression, MT_1 and MT_2 receptors exert opposite effects, with MT_1 receptors impairing and MT_2 receptors promoting cancer cell proliferation [15].

The search for novel classes of melatonin receptor ligands led us to design the versatile class of *N*-anilinoethylamides (Fig. 1) endowed with pharmacological properties that could be finely tuned according to specific substitutions in select positions [16]. Structure-activity relationship investigation brought to *N*-anilinoethylamides with agonist, partial agonist or antagonist behavior, as well as derivatives with improved physicochemical properties and metabolic stability [17,18]. To further characterize the structural requirements for melatonergic activity, the flexible *N*-anilinoethylamides were conformationally constrained by inscribing the ethylamide chain into a tetrahydroquinoline (THQ) nucleus, leading to 2-acylaminomethyl-THQ and 3-acylamino-THQ series which include some of the most potent MT_2-selective agonists [19,20]. We expected that the selection of active conformations through conformational constraints would lead to an increase of binding affinity. Additionally, the tetrahydropyridine ring thus obtained provided new positions amenable to insertion of substituents that could further modulate the pharmacological profile. We herein report a new class of melatonergic ligands derived from ring closure of the N-substituted-aniline portion of *N*-anilinoethylamides into a THQ nucleus, maintaining the flexible acylaminoethyl side chain (Fig. 1). Binding affinity and intrinsic activity of new compounds were modulated through select substitutions on the THQ nucleus and the amide side chain. These compounds were exploited to rationalize configurational and conformational aspects of ligand activity through molecular models that investigated dynamic properties of ligand-receptor interactions. Notably, replacement of the methoxy group with suitable polar substituents afforded new subtype-selective modulators with MT_1 agonist and MT_2 antagonist activity and antitumor activity in vitro and in vivo in a glioblastoma orthotopic xenograft model.

2. Chemistry

The (7-substituted-N-ethylamido)tetrahydroquinoline derivatives **3a-g** were prepared by reductive *N*-alkylation of the suitable 7-substituted-1,2,3,4-tetrahydroquinoline **2a-d** with *N*-(2,2-dimethoxyethyl)propionamide [21], [*N*-(2,2-dimethoxyethyl)-2,2-difluoroacetamide for **3f** or *N*-(2,2-dimethoxyethyl)acetamide for **3e** and **3g** [22] in the presence of triethylsilane (TES)/trifluoroacetic acid (TFA) (Scheme 1). The key starting 7-substituted-tetrahydroquinolines are commercially available (**2a**) or have been synthesized by *O*-alkylation of the commercially available 7-hydroxy-1,2,3,4-tetrahydroquinoline with 1-bromo-2-methoxyethane (for **2b**), 1-fluoro-3-iodopropane (for **2c**) or methyl chloroacetate (for **2d**), in the presence of NaH (Scheme 1).

The methyl ester derivatives **3d-f** were converted into the corresponding alcohols **4d-f** by reduction with $LiAlH_4$. On the other hand, the treatment of the ester derivative **3d** with a 2 N solution of ammonia in EtOH at room temperature gave the corresponding amido derivative **5**

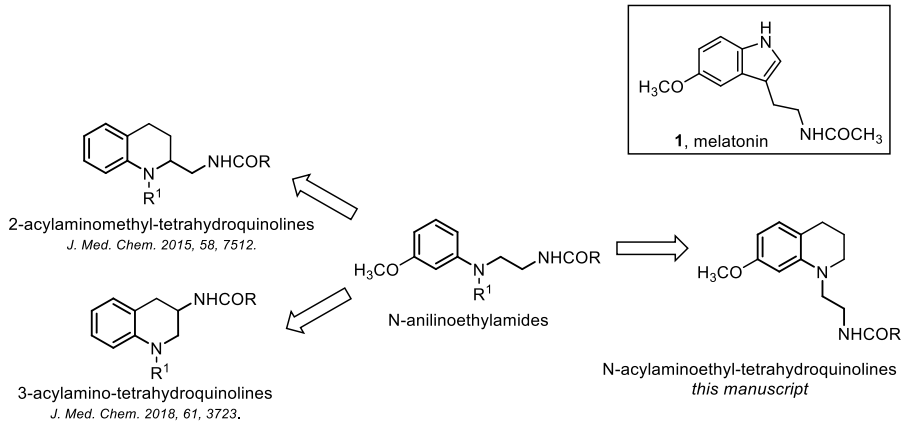
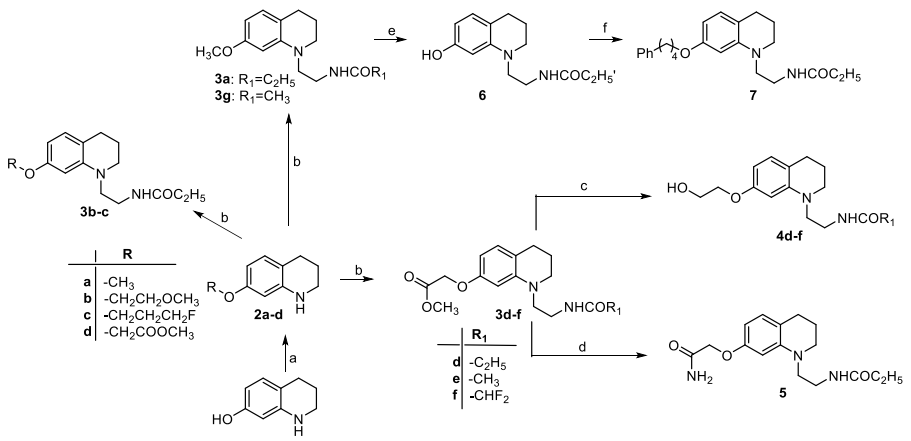


Fig. 1. Structure of melatonin and schematic representation of *N*-anilinoethylamide melatonin receptors ligands and derived conformationally constrained tetrahydroquinolines.



Scheme 1. Synthesis of (7-substituted-*N*-ethylamido)THQ derivatives **3a-c**, **3g**, **4d-f**, **5** and **7**. Reagents and conditions: a) 1-bromo-2-methoxyethane (for **2b**), 1-fluoro-3-iodopropane (for **2c**) or methyl chloroacetate (for **2d**), NaH 60 %, DMF, −10 °C to rt, 6 h, 62–70 %; b) *N*-(2,2-dimethoxyethyl)propionamide (for **3a-d**), *N*-(2,2-dimethoxyethyl)acetamide (for **3e** and **3g**) or *N*-(2,2-dimethoxyethyl)-2,2-difluoroacetamide (for **3f**), TES, TFA, DCM, rt, 2 h, 39–62 %; c) $LiAlH_4$, THF, 0 °C, 1h, 54–88 %; d) 2 N NH_3 in EtOH, rt, 24 h, 64 %; e) 1 M BBr_3, DCM, rt, 20 h, 74 %; f) NaH 80 %, 1-bromo-4-phenylbutane, DMF, rt, 6 h, 92 %.

(Scheme 1).

O-demethylation of **3a** with boron tribromide and subsequent *O*-alkylation of the intermediate phenol **6** with 1-bromo-4-phenylbutane in the presence of NaH, gave the desired 7-(4-phenylbutoxy) analog **7** (Scheme 1).

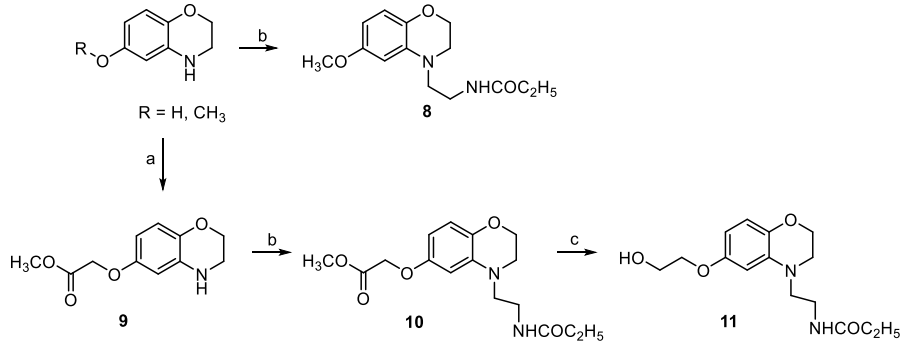
The 3,4-dihydro-2*H*-benzo[*b*][1,4]oxazine target compounds **8** and **11** were prepared using synthetic protocols similar to that above described and depicted in Scheme 2. In particular, **8** was obtained by reductive *N*-alkylation of commercially available 6-methoxy-3,4-dihydro-2*H*-benzo[*b*][1,4]oxazine with *N*-(2,2-dimethoxyethyl)propionamide in the presence of TES/TFA, whereas **11** was prepared by $LiAlH_4$ reduction of the intermediate methyl ester derivative **10** that, in turn, was prepared by *O*-alkylation of commercially available 3,4-dihydro-2*H*-benzo[*b*][1,4]oxazin-6-ol with methyl chloroacetate and subsequent reductive *N*-alkylation of methyl 2-[(3,4-dihydro-2*H*-benzo[*b*][1,4]oxazin-6-yl)oxy]acetate **9** with *N*-(2,2-dimethoxyethyl)propionamide in the presence of TES/TFA.

Similarly, the agomelatine analogue **13** was prepared by *O*-alkylation of *N*-[2-(7-hydroxynaphtalen-1-yl)ethyl]acetamide [23] with methyl chloroacetate in the presence of NaH and subsequent reduction of the ester intermediate **12** with $LiAlH_4$ (Scheme 3).

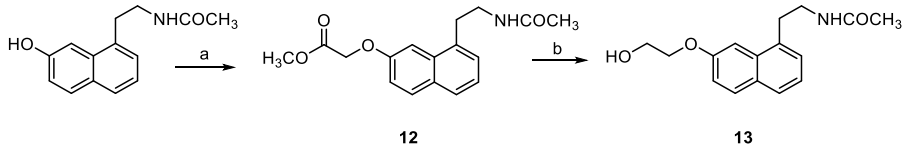
The synthetic approach shown in Scheme 4 was used for the preparation of the 2-mercaptoethoxy derivative **16**. In particular, the alcohol **4d** was subjected to the Mitsunobu reaction with thioacetic acid (AcSH) to give the thioester **14**, that was then converted into the disulfide intermediate **15** by treatment with sodium methoxide. The final reduction of the disulfide bond by treatment with tris(2-carboxyethyl)phosphine hydrochloride (TCEP) gave the desired 2-mercaptoethoxy target compound **16**.

The 2-substituted tetrahydroquinoline target derivatives **24a-b** were synthesized by *N*-cyanomethylation of the suitable 2-substituted-tetrahydroquinoline **22a-b** with bromoacetonitrile, followed by Raney nickel hydrogenation of the intermediate nitriles **23a-b** and concomitant *N*-acylation of the crude primary amines with propionic anhydride (Scheme 5). Since these synthetic steps do not involve chiral centers, the obtained products (*S*)- and (*R*)-**24a** retain the absolute configuration of the 2-substituted-tetrahydroquinolines (*S*)- and (*R*)-**22a**.

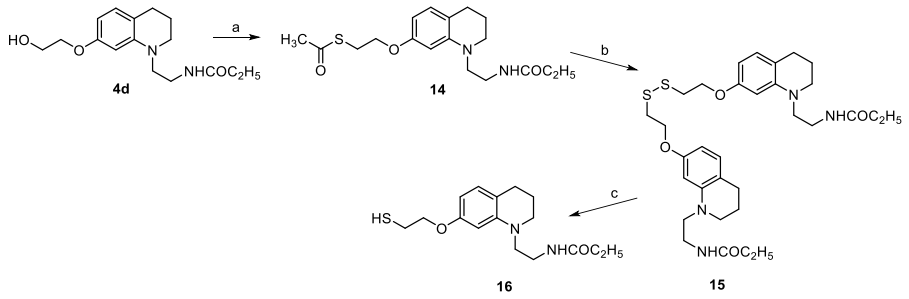
The key 2-methyl-7-methoxy-1,2,3,4-tetrahydroquinolines, in their racemic [(*R,S*)-**22a**] and optically active form [(*R*)-**22a** or (*S*)-**22a**], were in turn prepared through several steps starting from 4-iodo-3-nitroanisole (Scheme 5). Briefly, a Sonogashira cross-coupling between commercially available (*R,S*), (*R*)- or (*S*)-3-butyn-2-ol and 4-iodo-3-nitroanisole, followed by reduction of both nitro group and triple bond (H_2, 5 atm, Pd/C 10 %) of the derived nitroalkynes (*R,S*)-, (*R*)- or (*S*)-**17a**, and subsequent trifluoroacetylation of the resulting amino alcohols (*R,S*)-, (*R*)- or (*S*)-**18a**, gave a mixture of *N,O*-bis-(trifluoroacetylated) (**19a**) and *N*-trifluoroacetylated (**20a**) derivatives. Intermediates **19a** could be traced back to the corresponding alcohols (**20a**) by treatment with NaH at room temperature. Mesylation of the derived alcohols (*R,S*)-, (*R*)- and (*S*)-**20a** under classic conditions (MsCl, Py, DCM), and final cyclization through an intramolecular nucleophilic substitution in the presence of NaH (the latter reaction step takes place with Walden inversion at the chiral carbon atom), gave the 7-methoxy-2-methyl-tetrahydroquinolines (*R,S*)-, (*R*)- or (*S*)-**22a**. Instead, the racemic intermediate 7-methoxy-2-phenyl-1,2,3,4-tetrahydroquinoline (*R,S*)-**22b** was obtained by hydrogenation (5 atm, Raney-Ni) of 7-



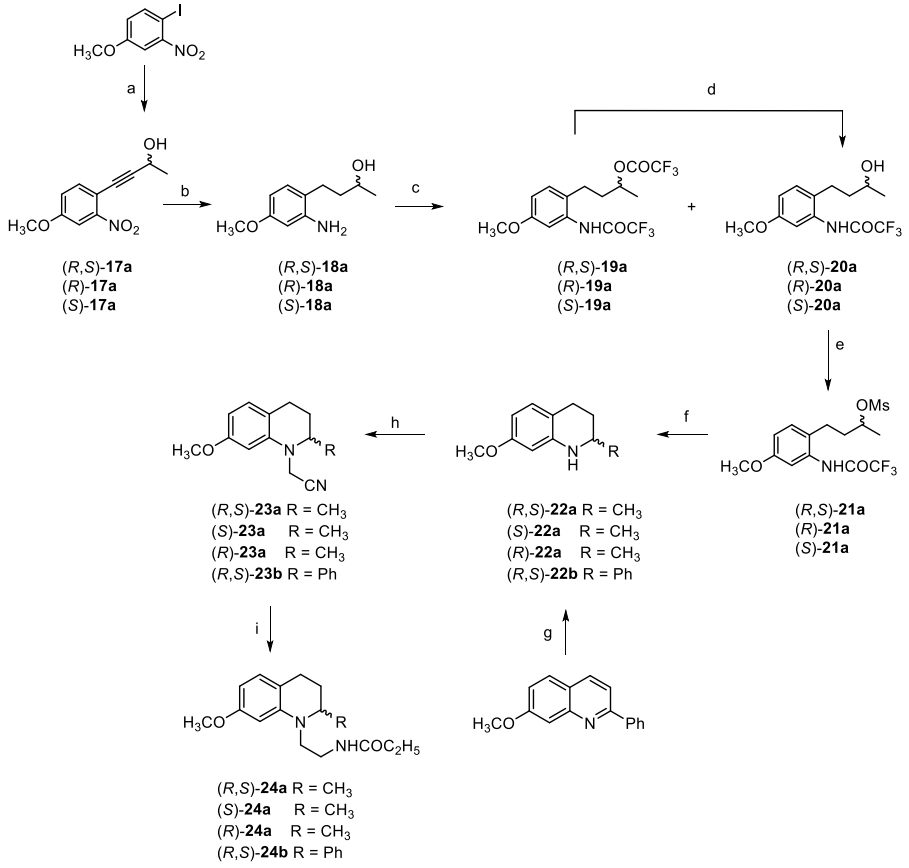
Scheme 2. Synthesis of benzo[*b*][1,4]oxazine target compounds **8** and **11**. Reagents and conditions: a) methyl chloroacetate, NaH 60 %, DMF, −10 °C to rt, 6 h, 73 %; b) *N*-(2,2-dimethoxyethyl)propionamide, TES, TFA, DCM, rt, 2 h, 29–52 %; c) $LiAlH_4$, THF, 0 °C, 1 h, 64 %.



Scheme 3. Synthesis of naphthalene derivative **13**. Reagents and conditions: a) methyl chloroacetate, NaH 60 %, DMF, −10 °C to rt, 6 h, 76 %; b) $LiAlH_4$, THF, 0 °C, 1 h, 77 %.



Scheme 4. Synthesis of 7-(2-mercaptoethoxy)THQ derivative **16**. Reagents and conditions: a) $P(Ph)_3$, diisopropyl azodicarboxylate (DIAD), AcSH, THF, 0 °C to rt, 18 h, 83 %; b) CH_3ONa, MeOH, rt, 16 h, 65 %; c) TCEP, acetate buffer, MeOH, 45 °C, 4 h, 81 %.

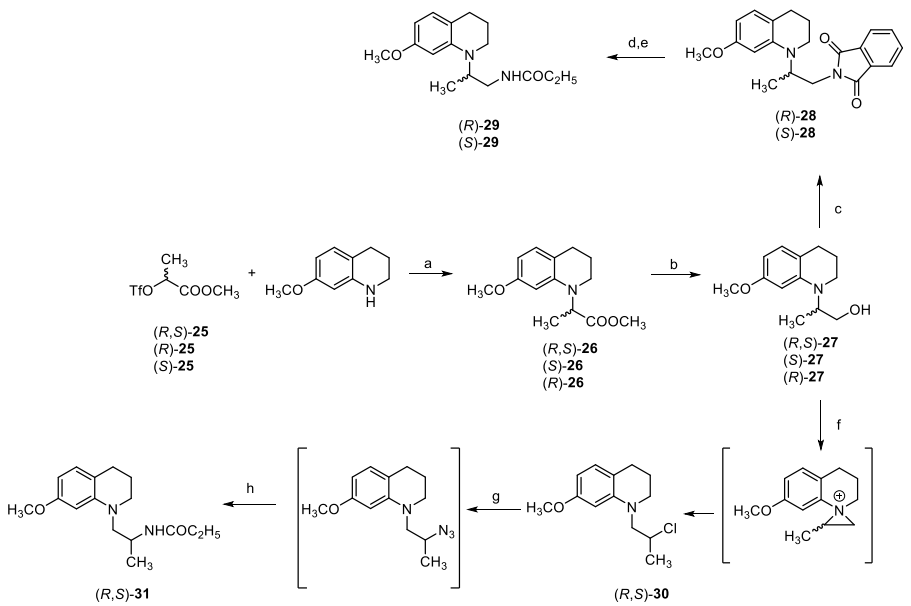


Scheme 5. Synthesis of 2-methy- and 2-phenyl-substituted THQ derivatives **24a-b**. Reagents and conditions: a) (*R*,*S*), (*R*) or (*S*)-but-3-yn-2-ol, $PdCl_2(PPh_3)_2$, CuI, Et_3N, 60 °C, 40 min, 70–88 %; b) H_2 (5 atm), Pd/C 10 %, EtOH, rt, 24 h, 66–92 %; c) trifluoroacetic anhydride, Et_3N, DCM, 0 °C, 15 min, 55 %; d) NaH 60 %, DMF, rt, 3 h, 85–90 %; e) MsCl, Py, DCM, rt, 16 h, 47–84 %; f) NaH 60 %, DMF, rt, 8 h, 65–90 %; g) H_2 (5 atm), Raney-Ni, THF, 60 °C, 6 h, 67 %; h) $BrCH_2CN$, DMF, 100 °C, 7 h for **23a** and $BrCH_2CN$, KI, K_2CO_3, DMF, 80 °C, 16 h for **23b**, 42–58 %; i) H_2 (4 atm), Raney-Ni, propionic anhydride, THF, 60 °C, 6 h, 65–96 %.

methoxy-2-phenylquinoline [24].

The two enantiomeric compounds (*S*)-**29** and (*R*)-**29** were prepared according to the synthetic sequence illustrated in Scheme 6.

N-alkylation of 7-methoxy tetrahydroquinoline with methyl (*R*,*S*)-(*S*)- or (*R*)-2-(trifluoromethylsulfonyloxy)propanoate (**25**) [25,26] (the reaction takes place with Walden inversion at the chiral carbon atom),

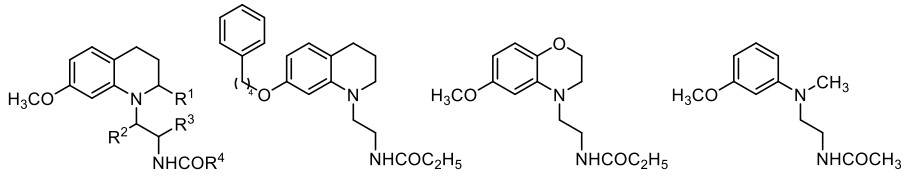


Scheme 6. Synthesis of THQ derivatives α- or β-methyl-substituted on the ethylamide side chain **31** and **29**. Reagents and conditions: a) 2,6-lutidine, CH_3CN, 70 °C, 16 h, 78–82 %; b) $LiAlH_4$, THF, rt, 1 h, 93–97 %; c) DCAD, phthalimide, PPh_3, THF, rt, 24 h, 47–52 %; d) $N_2H_4H_2O$, CH_3COOH, CH_3OH, reflux, 4 h; e) propionic anhydride, Et_3N, THF, rt, 1 h, two-step yield 76–81 %; f) MsCl, Et_3N, DCM, rt, 20 h, 37 %; g) NaN_3, DMF, 110 °C; 4 h; h) H_2 (4 atm), Pd/C 10 %, propionic anhydride, *i*-PrOH, rt, 6 h, two-step yield 55 %.

followed by $LiAlH_4$ reduction of the derived aminoesters (*R,S*)-, (*R*)- or (*S*)-**26**, gave the corresponding alcohols (*R,S*)-, (*R*)- or (*S*)-**27**. The two enantiomeric alcohols (*R*)- or (*S*)-**27** were made to couple with phthalimide by Mitsunobu reaction in the presence of triphenyl phosphine and di-*p*-chlorobenzyl-azodicarboxylate (DCAD) to form the corresponding phthalimido derivatives (*R*)-**28** or (*S*)-**28.** Hydrazinolysis of these phthalimido intermediates and subsequent *N*-acylation of the corresponding crude amine with propionic anhydride afforded the desired melatonin ligands (*R*)-**29** or (*S*)-**29** (enantiomeric purity 84 % and 95 % respectively, determined by chiral HPLC).

The target compound (*R,S*)-**31** was synthesized through a synthetic sequence involving the reaction of alcohol (*R,S*)-**27** with mesyl chloride to give (with the intermediation of an aziridinium species [27]) the secondary chloride (*R,S*)-**30** as the major regioisomer; subsequent treatment of (*R,S*)-**30** with NaN_3 provided an azido intermediate that was converted into the desired final compound (*R,S*)-**31** by catalytic

Table 1
Binding affinity and intrinsic activity of *N*-acylaminoethyl-tetrahydroquinolines at human melatonin receptors MT_1 and MT_2.



3a,g, 24a, 24b, 29, 31 **7** **8** **UCM793**

Compd.	R [1]	R [2]	R [3]	R [4]	hMT_1		hMT_2	
					$pK_i \pm SD$[a]	$IA_r \pm SD$[b]	$pK_i \pm SD$[a]	$IA_r \pm SD$[b]
1,melatonin					9.60 ± 0.18	1.00 ± 0.09	9.44 ± 0.12	1.00 ± 0.07
UCM793[c]					8.76	0.95	8.65	1.06
3a	H	H	H	C_2H_5	8.88 ± 0.02	0.96 ± 0.04	9.59 ± 0.18	0.99 ± 0.04
3g	H	H	H	CH_3	9.02 ± 0.10	1.03 ± 0.10	9.51 ± 0.12	1.01 ± 0.10
7					7.38 ± 0.08	nd	6.80 ± 0.05	nd
8					8.74 ± 0.12	0.96 ± 0.15	9.16 ± 0.26	1.04 ± 0.07
(*R,S*)-**24a**	CH_3	H	H	C_2H_5	8.06 ± 0.03	0.98 ± 0.04	8.71 ± 0.05	0.95 ± 0.09
(*R*)-**24a**	CH_3	H	H	C_2H_5	8.22 ± 0.05	0.95 ± 0.14	8.50 ± 0.17	0.83 ± 0.10
(*S*)-**24a**	CH_3	H	H	C_2H_5	7.74 ± 0.04	0.93 ± 0.08	8.82 ± 0.21	1.12 ± 0.15
(*R,S*)-**24b**	Ph	H	H	C_2H_5	6.63 ± 0.07	0.60 ± 0.20	7.43 ± 0.07	0.81 ± 0.06
(*R*)-**29**	H	CH_3	H	C_2H_5	8.23 ± 0.01	0.95 ± 0.10	8.53 ± 0.14	0.94 ± 1.00
(*S*)-**29**	H	CH_3	H	C_2H_5	8.91 ± 0.20	0.71 ± 0.06	9.13 ± 0.26	0.88 ± 0.03
(*R,S*)-**31**	H	H	CH_3	C_2H_5	6.99 ± 0.01	nd	7.16 ± 0.09	nd

[a] pK_i values were calculated from IC_{50} values, obtained from competition curves by the method of Cheng and Prusoff [34], and are the mean of at least three determinations performed in duplicate.

[b] The relative intrinsic activity values were obtained by dividing the maximum analogue-induced G protein activation by that of melatonin. Measurements were performed in triplicate. nd: not determined.

[c] Binding affinity and intrinsic activity values taken from ref. 28.

hydrogenation (4 atm, Pd/C 10 %) and concomitant acylation of the crude alkylamine with propionic anhydride (Scheme 6). The observed NH-CH_α-CH_3 correlation in the COSY spectrum is in agreement with the proposed structure of compound (*R,S*)-**31** (Supplementary Material Fig. S1).

3. Results and discussion

3.1. Structure-activity relationships

N-Acylaminoethyl-THQs were decorated with substituents on the THQ nucleus and on the amide side chain to evaluate their ability to behave according to structure-activity relationships established for melatonergic ligands. Therefore, acetyl and propionyl amides were synthesized, as well as methylated derivatives on carbon atoms of the side chain. Substituents favoring subtype selectivity were also considered, such as a phenylbutoxy replacing the methoxy group and a methyl or phenyl ring in position 2. These structural modifications should, in principle, enhance MT_1 or MT_2 binding affinity, respectively. The methoxy derivatives **3g** and **3a** showed nanomolar binding affinities (Table 1), similar to that of the *N*-anilinoethylamide UCM793 at the MT_1 receptor and with a moderate increase at the MT_2 receptor. Compared to melatonin, **3g** and **3a** maintained binding affinity at the MT_2 receptor but were less potent at the MT_1 receptor and behaved as full agonists at both receptors. Insertion of an oxygen atom in the benzo-oxazine derivative **8** slightly reduced potency and MT_2 selectivity. Binding affinity was modulated by applying substitution patterns derived from other ligands. As observed for *N*-anilinoethylamides [28], insertion of a methyl group on carbon β of the ethylamide side chain led to the (*S*)-**29** having higher binding affinity than (*R*)-**29** enantiomer at both receptor subtypes. Methylation of carbon α of the ethylamide side chain in (*R, S*)-**31** was not tolerated and produced a pronounced decrease in binding affinity. Replacement of the methoxy substituent with a 4-phenylbutoxy group (**7**) inverted receptor subtype selectivity, as seen for several MT_1-selective ligands reported in literature in which a bulky, lipophilic substituent was introduced in the position corresponding to that of the methoxy group [29–31]. Looking for compounds with greater MT_2-selectivity, we also investigated 2-substituted THQs that could occupy the "out-of-plane" region associated with MT_2 selectivity [32]. Limited information is available on the effect of substituents on the atom close to the amide chain of ligands with a benzo-fused six-membered cycle, essentially coming from tetralin derivatives [33]. A methyl group produced a drop in binding affinity of similar entity ($\Delta pK_i \approx 0.8$) at MT_1 and MT_2 receptors which displayed different tolerance, with the MT_1 receptor better accommodating (*R*)-**24a** and the MT_2 receptor (*S*)-**24a**. 2-Phenyl derivatives (*R,S*)-**24b** showed a more pronounced decrease of binding affinity, with limited MT_2-selectivity.

3.2. Molecular modelling

Molecular models were used to investigate structure-activity relationships observed for THQ derivatives. In particular, the role of the THQ scaffold in the interaction with binding site residues in comparison with the *N*-anilinoethylamide counterpart was investigated through thermodynamic integration simulations. Molecular dynamics was applied to study the effect on conformational equilibria and receptor recognition of the insertion of a methyl group on the THQ nucleus and on the ethylamide side chain.

3.2.1. Free energy estimation of tetrahydroquinoline selectivity for the MT_2 receptor

Compared with the nonselective UCM793, compound **3g** showed a moderate selectivity for the MT_2 receptor deriving from better accommodation at the MT_2 receptor. To investigate the ability of molecular models of ligand-receptor complexes to account for differences in experimental MT_1 and MT_2 receptor binding affinities, single-step thermodynamic integration (TI) simulations [35] were performed to alchemically transform the THQ derivative **3g** into the nonselective UCM793. To this end, the THQ ring of **3g** bound within the MT_1 or MT_2 receptor binding site was transformed into the *N*-methylaniline of UCM793 and the difference in free-energy changes at the two receptors was calculated. To account for the effect of the starting configuration on the result of TI calculations, four independent simulations were carried out for each receptor complex, starting from different snapshots obtained from a preliminary molecular dynamics simulation of the MT_1 or MT_2-**3g** complex. In TI simulations, Coulomb and van der Waals potentials of unique atoms in **3g** and UCM793 (Fig. S2) were replaced with λ-dependent softcore potentials [36]. The coupling parameter λ, which varies from 0 to 1, accounts for the transformation of the THQ ring of **3g** (corresponding to $\lambda = 0$) into the *N*-methylaniline of UCM793 ($\lambda = 1$). Fig. 2 represents compound **3g** at the beginning of the transformation ($\lambda \approx 0.0092$, a value at which softcore atom potentials mostly approximate the ones of **3g**) and UCM793 obtained at the end of the transformation ($\lambda \approx 0.9978$, a value at which softcore atom potentials mostly approximate the ones of UCM793) in the MT_1 and MT_2 binding site. The simulations were arranged in a thermodynamic cycle (Fig. S3) that provided a ΔΔG value related to the selectivity of **3g** for the MT_2 receptor. The same alchemical transformations were not performed in solvent since it would be the same for both receptors and irrelevant for free-energy difference calculations related to receptor subtype selectivity. For each simulation, the integration of $\langle \partial V/\partial \lambda \rangle$, i.e., the expectation of the derivative of the potential energy over the coupling parameter λ, gave free-energy difference profiles (Fig. S4) that were averaged for each receptor. At the end of the alchemical transformation, ($\lambda = 1$, corresponding to the presence of UCM793 in the binding site), positive ΔG values of 0.45 kcal/mol at the MT_1 receptor and a greater one of 1.10 kcal/mol at the MT_2 receptor were recorded. The overall $\Delta\Delta G_{calc}(MT_2\text{-}MT_1) = 0.65 \pm 0.22$ kcal/mol agrees with the experimental $\Delta\Delta G_{exp} = 0.82$ kcal/mol and supports the better accommodation of THQ **3g** at the MT_2 receptor, albeit with a moderate selectivity. The higher MT_2 binding affinity of compound **3g** is likely related to the larger MT_2 binding pocket as revealed by crystal structures analysis [37]. A similar moderate MT_2 selectivity has been reported for [2-(1,2,3,4-tetrahydronaphthalen-1-yl)ethyl]acetamide having a tetralin scaffold [38]. Analysis of amino acids surrounding the co-crystallized agonist in MT_1 and MT_2 receptors reveals elevated sequence identity (Fig. S5), with conserved ligand-interacting residues. The larger MT_2 binding site is mainly due to conformational differences in residue side chains. In particular, a major cause for the larger volume in front of the pyrrole portion of melatonin is the presence of a different amino acid in position 7.40. The bulky MT_1 tyrosine ($Tyr282^{7.40}$), compared with $Leu295^{7.40}$ in the MT_2 receptor, prompts a more pronounced entrance of adjacent Tyr7.39 (MT_1 Tyr281, MT_2 Tyr294) and Tyr7.43 (MT_1 Tyr285, MT_2 Tyr298) within the binding site than in the MT_2 receptor [39]. This larger MT_2 subpocket likely allows better accommodation of the tetrahydropyridine portion of *N*-acylaminoethyl-THQs, leading to the observed moderate MT_2 selectivity.

3.2.2. Arrangement of 2-methyl group affects receptor binding affinity

The substituent in position 2 of the THQ scaffold was expected to occupy a region of the receptor where bulky substituents (e.g., phenyl, naphthyl, benzyl) are tolerated, potentially leading to an increase in binding affinity and MT_2 selectivity. However, both the methyl (**24a**) and the phenyl (**24b**) substituents showed reduced potency. To rationalize the decreased affinity, the enantiomers of **24a** were docked into MT_1 and MT_2 binding site. (*R*)-**24a** and (*S*)-**24a** established polar

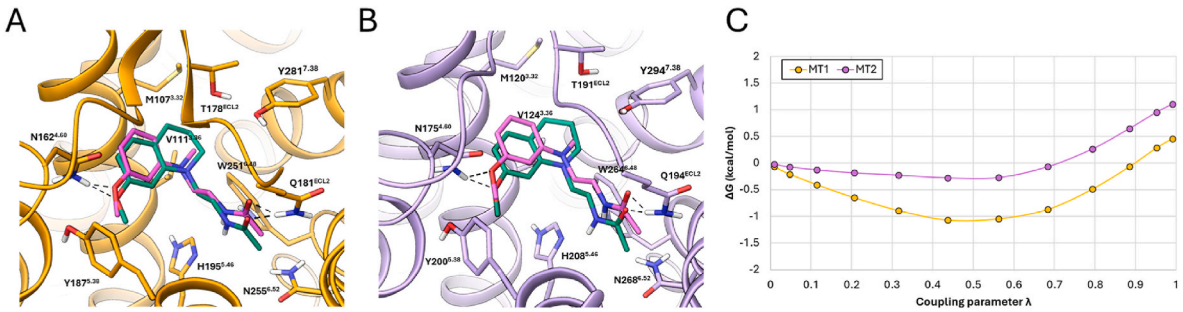


Fig. 2. A, B) Representative snapshots of thermodynamic integration simulations showing **3g** (green, $\lambda = 0.0092$) and UCM793 (pink, $\lambda = 0.9978$) within the binding site of MT_1 (orange, panel A) and MT_2 (purple, panel B) receptors. C) Free-energy profiles calculated from thermodynamic integration simulations: ΔG values were retrieved at different λ values during the alchemical transformation of **3g** into UCM793 within the MT_1 (orange line and dots) and MT_2 (purple line and dots) receptors. (For interpretation of the references to color in this figure legend, the reader is referred to the Web version of this article.)

interactions with binding site residues, i.e., hydrogen bonds between the methoxy oxygen and Asn162/175$^{4.60}$ in transmembrane helix (TM) 4 and between the side chain carbonyl and Gln181/194 in extracellular loop 2 (ECL2). Additionally, the phenyl ring of the THQ scaffold formed a π-stacking interaction with Phe179/192 in ECL2. The binding mode is consistent with that observed for agonists co-crystallized with MT_1 and MT_2 receptors [2].

The favorite poses obtained for (*R*)-**24a** and (*S*)-**24a** were characterized by the methyl group in an axial arrangement at both receptors (Fig. S6). The stability of the binding poses was confirmed by molecular dynamics (MD) simulations. During 200 ns-long MD, the orientation of the methyl group selected by the docking procedure remained largely preferred (Fig. 3). In the case of (*R*)-**24a**-MT_1, (*S*)-**24a**-MT_1 and (*S*)-**24a**-MT_2 complexes, for which no conformational changes of the THQ nucleus were observed, MD simulations were repeated starting from conformations with equatorial methyl group. After a short time, ligand conformation shifted to the axial methyl arrangement which was maintained till the end of the simulation (Fig. S7).

To investigate the axial/equatorial preference of the substituent in position 2, NMR experiments were performed for compounds **24a** and **24b** dissolved in chloroform. ^{1}H NMR spectra supported a large prevalence of the methyl axial arrangement (Fig. S8). This conformational preference was properly reproduced by our computational protocol. 2-μs-long MD simulation of (*S*)-**24a** in a box of explicit chloroform resulted in a largely preferred axial arrangement. A similar axial conformational abundance was predicted in water (Fig. S9).

Given the preferred axial arrangement, the methyl group does not occupy the region of the binding site reached by substituents in position 2 of indole ligands which show an increased potency. Investigation of ligand-receptor complexes allowed us to identify the close proximity of the axial methyl group of (*R*)-**24a** with the side chain of Tyr281/294$^{7.38}$, and of the axial methyl group of (*S*)-**24a** with Val111/124$^{3.36}$ in the MT_2 receptor as the likely reason for the observed reduction of binding affinity brought by insertion of a substituent in position 2 of the THQ nucleus (Fig. S6). In fact, melatonergic ligands are characterized by a core scaffold with a reduced transverse cross-section, smaller than the one generated by the axial methyl group which is oriented roughly perpendicular to the THQ ring.

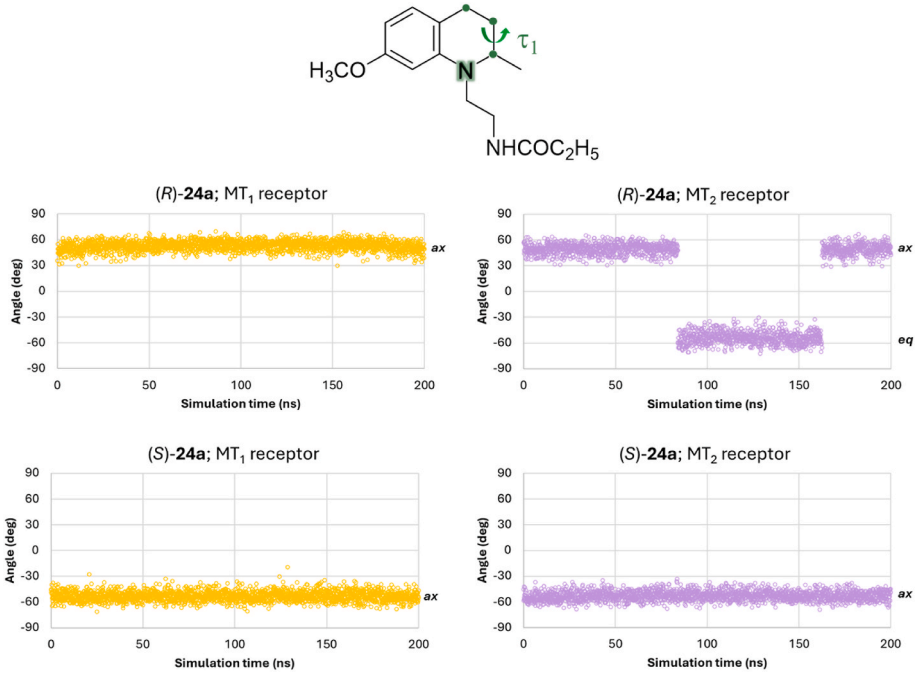


Fig. 3. Values of dihedral angle τ1 monitored during 200 ns of MD simulation for (*R*)-**24a** and (*S*)-**24a** in complex with the MT_1 and MT_2 receptors. *Ax* and *eq* indicate the values of dihedral angle τ1 corresponding to an axial or an equatorial arrangement of the methyl substituent, respectively.

3.2.3. Conformational enrichment explains receptor chiral recognition of (S)-29 and (R)-29

Introduction of a methyl group on carbon β of the ethylamide side chain, close to the THQ scaffold, differently affected binding affinity, depending on the stereochemistry of the chiral carbon. (*S*)-**29** was more potent than (*R*)-**29** at both receptors. We investigated if the difference in binding affinity between the two enantiomers could be ascribed to a higher abundance in solution of the binding conformations assumed by the eutomer (*S*)-**29**. A similar behavior had already been observed for β-methyl-substituted-*N*-anilinoethylamides. In this case, the methyl group altered the conformational equilibria of the unsubstituted side chain and induced an enrichment of the conformations observed in docking poses for the eutomer, while conformations assumed by the distomer bound to the receptor were disfavored [28]. To this end, (*S*)-**29** and (*R*)-**29** were docked into the MT_2 receptor binding site. The methyl group of both enantiomers occupies the lipophilic pocket located at the bottom of the ligand binding site, surrounded by residues Trp264$^{6.48}$, Val204$^{5.42}$, Val124$^{3.36}$, and Ile125$^{3.37}$ (Fig. S10). Distinct conformations of the ethylamide side chain allow accommodation of the methyl group. (*S*)-**29** side chain assumes dihedral angles τ1 (C8a-N-Cβ-Cα) = −159° and τ2 (N-Cβ-Cα-Namide) = 156°, and (*R*)-**29** τ1 = −61° and τ2 = −159° (see Fig. 4 for angle definitions). To access the available conformational space of (*S*)-**29** and (*R*)-**29** in solution, a 2-μs-long MD simulation of (*S*)-**29** in a box of explicit water molecules was conducted. The free energy surface (FES) obtained for (*S*)-**29** as a function of torsional angles τ_1 and τ_2, and the specular one corresponding to the FES of (*R*)-**29** are depicted in Fig. 4. The side chain conformation of the eutomer (*S*)-**29** docked into the MT_2 receptor corresponds to a free energy minimum, indicated by the green star in Fig. 4; on the contrary, the docked conformation of (*R*)-**29** does not correspond to any energy minimum. This result supports the conformational enrichment of the ligand conformations able to bind the receptor as the reason for the moderate stereoselectivity observed for β-methyl-THQ derivatives. To investigate if the results obtained from molecular dynamics simulations could be affected by the nature of the solvent (i.e., water) not considering the physiological ionic strength, we performed another 2-μs-long MD simulation of (*S*)-**29** in a box of solvent reproducing the same ionic strength as the extracellular compartment [40]. No change in (*S*)-**29** energy minima operated by the presence of ions was observed (Fig. S11).

3.3. Subtype-selective modulators of melatonin receptors

Binding affinities of *N*-acylaminoethyl-THQs could be modulated according to structure-activity relationships for melatonergic ligands and rationalized with theoretical models of receptor-ligand interaction. The new series provided compounds with limited MT_2 selectivity. On the other hand, a ligand with similar MT_1 and MT_2 binding affinities could be a suitable starting point for the preparation of compounds with different behavior at the two receptors, i.e., agonist at one subtype and antagonist at the other one. We therefore exploited the THQ nucleus and known structure-activity relationships to investigate mixed agonist-antagonist behavior.

5-HEAT (Table 2) is a 5-(2-hydroxyethoxy)indole derivative with the ability to selectively activate the MT_1 receptor while acting as an antagonist at the MT_2 subtype. Compared to melatonin, the hydrophilic side chain, replacing the methoxy group, reduces binding affinity by about one hundred times [41]. The peculiar behavior makes 5-HEAT a useful pharmacological tool to dissect the distinct effects of MT_1 and MT_2 activation and can represent a starting point for the development of novel treatments for pathologies in which MT_1 and MT_2 receptors play an opposite role (see Introduction). Attempts to obtain 5-HEAT analogs with improved potency were unsuccessful as introduction of different groups in position 5 of the indole ring could improve binding affinity but failed to replicate the MT_1/MT_2 differential intrinsic activity of 5-HEAT [42]. We therefore used the versatile THQ nucleus as a new scaffold to obtain more potent MT_1 agonist/MT_2 antagonist compounds by inserting a hydroxyethoxy chain in position 7, as well as a series of strict structural analogs of the hydroxyethoxy chain. We selected polar substituents with similar size as potential bioisosteres to maintain, or enhance, the different intrinsic activity and provide information about interactions and role of the substituent. Additionally, a difluoroacetamide side chain was also evaluated as it was shown to increase binding affinity on naphthalenic ligands [43,44]. Compounds **4e** and **4d** showed different intrinsic activities at MT_1 and MT_2 receptors, with higher binding affinity observed for the propionyl derivative compared to the acetyl one. Compound **4d** is characterized by the same intrinsic activity profile as 5-HEAT and higher binding affinity at both receptor subtypes. The benzo-oxazine scaffold was not as good, as compound **11** showed both lower binding affinity and difference in MT_1 and MT_2 intrinsic activity. Compound **4f** carrying the difluoroacetamide side

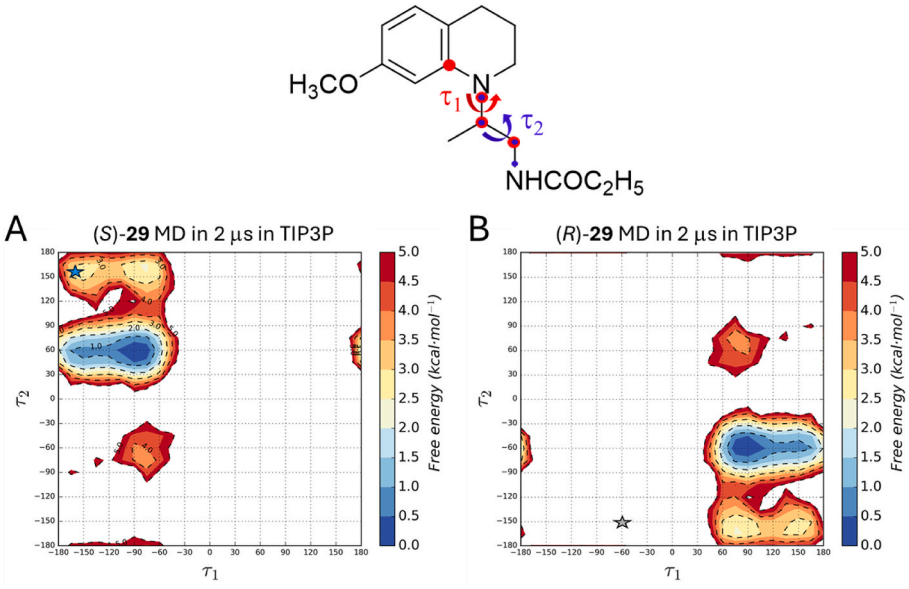
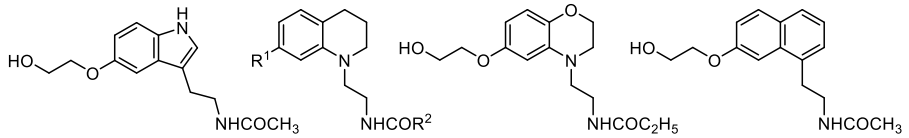


Fig. 4. Top: definition of τ_1 and τ_2 angles used for free energy calculation. Bottom left: free energy surface obtained for (*S*)-**29** after 2 μs of molecular dynamics simulation in a box of explicit water molecules. Bottom right: representation of the FES of (*R*)-**29**, obtained from that of (*S*)-**29** with opposite values of τ_1 and τ_2 angles. The marker (star) indicates τ_1 and τ_2 values associated with docking poses of (*S*)-**29** and (*R*)-**29**.

Table 2
Binding affinity and intrinsic activity of 7-substituted *N*-acylaminoethyl-tetrahydroquinolines and analogs.



5-HEAT | **3b,c, 4d-f, 5, 11, 16** | **11** | **13**

Compd.	R [1]	R [2]	hMT_1		hMT_2	
			$pK_i \pm SD$[a]	$IA_r \pm SD$[b]	$pK_i \pm SD$[a]	$IA_r \pm SD$[b]
5-HEAT			7.46 ± 0.11	0.57 ± 0.062	7.34 ± 0.07	0.11 ± 0.08
3b	$O(CH_2)_2OMe$	C_2H_5	7.63 ± 0.13	0.77 ± 0.10	7.99 ± 0.07	0.70 ± 0.07
3c	$O(CH_2)_3F$	C_2H_5	8.05 ± 0.15	0.78 ± 0.05	8.27 ± 0.06	0.82 ± 0.05
4d,UCM1400	$O(CH_2)_2OH$	C_2H_5	7.94 ± 0.07	0.42 ± 0.05	8.11 ± 0.06	0.06 ± 0.10
4e	$O(CH_2)_2OH$	CH_3	7.06 ± 0.08	0.44 ± 0.08	7.18 ± 0.05	0.25 ± 0.07
4f	$O(CH_2)_2OH$	CHF_2	7.62 ± 0.14	0.46 ± 0.06	8.11 ± 0.05	0.09 ± 0.08
5	OCH_2CONH_2	C_2H_5	6.65 ± 0.19	0.34 ± 0.05	7.03 ± 0.09	0.18 ± 0.05
11			7.06 ± 0.08	0.44 ± 0.08	7.18 ± 0.05	0.25 ± 0.07
13			8.33 ± 0.08	0.48 ± 0.06	8.47 ± 0.07	0.15 ± 0.13
16	$O(CH_2)_2SH$	C_2H_5	7.65 ± 0.14	0.58 ± 0.08	7.97 ± 0.24	0.69 ± 0.07

[a] pK_i values were calculated from IC_{50} values, obtained from competition curves by the method of Cheng and Prusoff [34] and are the mean of at least three determinations performed in duplicate.
[b] The relative intrinsic activity values were obtained by dividing the maximum analogue-induced G protein activation by that of melatonin. Measurements were performed in triplicate.

chain showed no increase in binding affinity and no change in the intrinsic activity profile compared to **4d**. Methylation of the hydroxyl group in position 7 (**3b**) or replacement with a thiol (**16**) or CH_2F group (**3c**) produced a significant increase in intrinsic activity at both receptors, abolishing the differential behavior at the two receptor subtypes. Amide derivatization (**5**) gave the greatest reduction of binding affinity. Interestingly, the differential modulation of intrinsic activity exerted by the hydroxyethoxy substituent does not appear to depend on the specific scaffold of the melatonergic ligand, as a result consistent with what observed for compound **4d** and 5-HEAT was obtained through decoration of the naphthalene nucleus of agomelatine (**13**).

Based on these results, we then investigated whether the hydroxyethoxy derivatives, i.e., the indole 5-HEAT and the THQ **4d**, also showed different functional behaviors at MT_1 and MT_2 receptors on cAMP assays, in comparison with the methoxy derivatives melatonin and **3g**. In forskolin-stimulated MT_1-and MT_2-expressing cells, all tested ligands modulated cAMP levels with distinct potency and efficacy profiles. Melatonin behaved as a full agonist at both receptors and was used as the reference for intrinsic activity (Table 3). **3g** showed a full agonistic profile and very high potency at both MT_1 and MT_2 receptors. Both **4d** and 5-HEAT showed near-full agonism at MT_1 with efficacy slightly below that of melatonin, but, interestingly, only minimal activity at MT_2. Consistent with its very low intrinsic activity, the

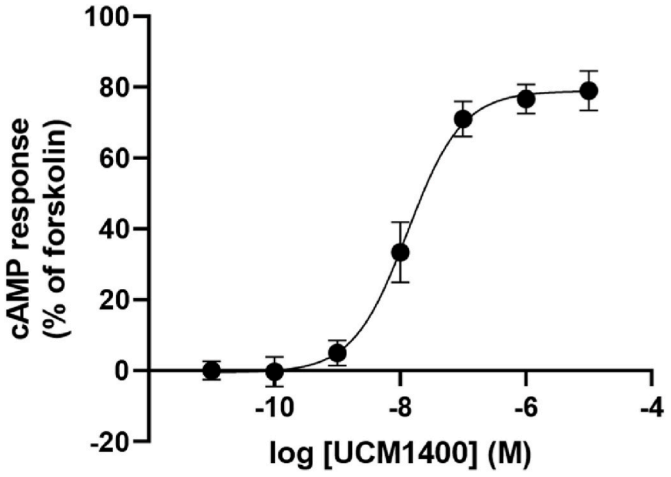


Fig. 5. Dose–response curve of compound **4d** (UCM1400) on melatonin-induced inhibition of forskolin-stimulated cAMP accumulation in hMT_2 cells. cAMP levels were normalized to the forskolin (1 μM) response (100 %), with 0 % representing the melatonin (1 nM)-induced inhibition. Data represent mean ± SEM of n = 3 independent experiments.

Table 3
Relative intrinsic activity (IA_r)[a] and potency (pIC_{50})[b] and of ligands at human melatonin receptors MT_1 and MT_2 in cAMP assays.

Compd.	Intrinsic activity		Agonist potency		Antagonist potency
	hMT_1	hMT_2	hMT_1	hMT_2	hMT_2
	$IA_r \pm SD$	$IA_r \pm SD$	$pIC_{50} \pm SD$	$pIC_{50} \pm SD$	$pIC_{50} \pm SD$
1,melatonin	1.00 ± 0.05	1.00 ± 0.06	9.53 ± 0.07	9.02 ± 0.08	
5-HEAT	0.83 ± 0.07	0.13 ± 0.04	7.62 ± 0.05		7.43 ± 0.10
3g	0.97 ± 0.06	1.04 ± 0.04	9.20 ± 0.04	9.75 ± 0.07	
4d,UCM1400	0.73 ± 0.05	0.18 ± 0.05	8.22 ± 0.06		7.87 ± 0.12

[a] Intrinsic activity values were calculated relative to the maximal effect of melatonin (set as 1.00), with all compounds tested in the presence of 1 μM forskolin. Data represent mean ± SD from n = 3 independent experiments.
[b] pIC_{50} values refer to the negative logarithm of the concentration producing 50 % of the maximal effect on the reduction of forskolin (1 μM)-stimulated cAMP levels, except for 5-HEAT and **4d** on MT_2 where pIC_{50} values refer to the negative logarithm of the concentration producing 50 % restoration of forskolin (1 μM)-stimulated cAMP from melatonin (1 nM)-induced inhibition.

antagonistic behavior of **4d** at MT_2 is further demonstrated by the dose-response curve showing the inhibition of melatonin-induced cAMP reduction (Fig. 5).

3.4. 3a and 4d (UCM1400) differently affect the MT_2, but not MT_1, receptor conformation

To investigate the dynamic behavior of MT_1 and MT_2 receptors in complex with the subtype-selective mixed agonist-antagonist **4d**, 2 μs-long MD simulations were performed. The effect produced by **4d** was compared with that of the agonist **3a**, which bears an analogous ethylamide side chain but a methoxy group instead of the hydroxyethoxy chain. Principal component analysis (PCA) [45] of the Cα atomic coordinates from the last 1.5 μs of the four MD trajectories revealed clearly distinct distributions of frames along the first principal component (PC1) for MD simulations of **4d** and **3a** bound to the MT_2 receptor and an overall overlapping distribution of conformational states for MT_1 complexes with the two ligands (Fig. 6A). Analysis of the sum of squared loadings for PC1 from a PCA conducted on trajectories of the MT_2 receptor complexes enabled the evaluation of the residue-wise contribution to the protein motions (Fig. 6B). The receptor region close to the terminal CH_2OH group of the 2-hydroxyethoxy substituent—encompassing portions of TM4 and TM5—exhibited relatively high values of the sum of squared loadings, especially in the case of TM5 residues (Fig. 6B and C). Additional regions of the protein also showed elevated contributions. Notably, domains not in direct contact with the ligand but located near the receptor–G protein interface, such as the central portion of TM5, intracellular loop 3 (IL3), and the initial segment of TM6, highly contributed to the motions captured by PC1, indicating that these regions play a major role in defining the conformational differences between the MT_2-**3a** and MT_2-**4d** complexes along PC1 (Fig. 6C). Taken together, these results suggest that binding of the subtype-selective modulator **4d** induces perturbations in regions of the MT_2 receptor not limited to the orthosteric binding site, but also in close proximity to the G-protein interaction interface, promoting conformational changes distinct from those elicited by the agonist **3a**.

*3.5. MT_1 agonist-MT_2 antagonist **4d** (UCM1400) exerts anti-tumor effect*

We investigated the effects of **4d** (UCM1400), a compound that selectively activates MT_1 and inhibits MT_2 receptors, a mechanism previously shown to exert anti-tumor effects in vitro and in vivo [15]. Our results demonstrate that UCM1400 treatment dose-dependently reduced the proliferation of HOG (Fig. 7A) and U87MG (Fig. 7B) human glioma cell lines. Furthermore, continuous infusion of UCM1400 for 14 days inhibited orthotopic U87MG tumor growth by

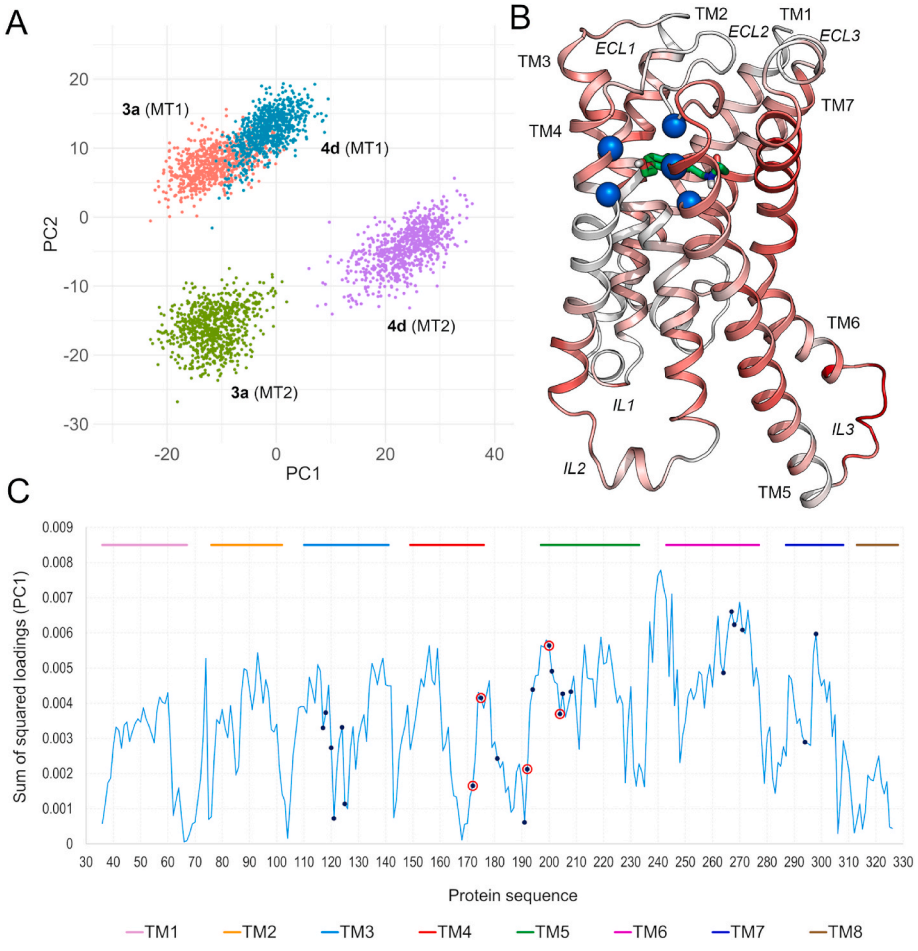


Fig. 6. (A) PCA score plot showing the distribution of frames of MD simulations of MT_1 and MT_2 receptors in complex with **3a** and **4d** (sampled every 2 ns from the final 1.5 μs of each simulation) projected onto PC1 and PC2. Colored dots correspond to different ligand-protein complexes (cyan: **4d**–MT_1; orange: **3a**–MT_1; violet: **4d**–MT_2; green: **3a**–MT_2). **(B)** Model of **4d** (green carbon atoms) docked within MT_2 receptor (PDB ID: 7VH0); blue spheres indicate Cα of residues within 3.5 Å of the terminal CH_2OH group of the 2-hydroxyethoxy substituent. Protein residues are colored by their contribution to the motions described by PC1, calculated as the sum of squared loadings of Cα atoms, with white and red indicating minimal and maximal contribution, respectively. **(C)** Residue-wise contribution to PC1 for MT_2 receptor MD simulations (cyan trace), calculated as the sum of squared loadings of Cα atoms. Colored bars indicate the position of transmembrane helices; blue dots indicate residues within 3.5 Å of the ligand, and red-circled dots indicate residues within 3.5 Å of the terminal CH_2OH group of the 2-hydroxyethoxy substituent. (For interpretation of the references to color in this figure legend, the reader is referred to the Web version of this article.)

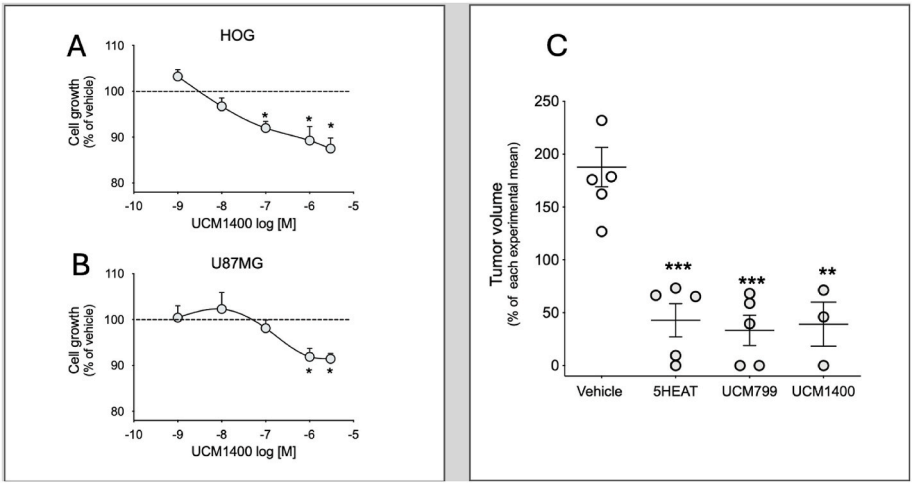


Fig. 7. UCM1400-induced simultaneous activation of MT_1 and inhibition of MT_2 receptors impairs glioma growth in vitro and in vivo. (**A** and **B**) High (HOG) and Low (U87MG) melatonin glioma cell lines were cultured for 48 h with UCM1400 (10^{-9} – 3.10^{-6} M) or the respective vehicle (2×10^{-6} – 2×10^{-3} % DMSO). Cell number was estimated by MTT assay, and values were normalized by the mean absorbance detected in the respective vehicle group. Data are shown as mean ± SEM of four independent experiments in quadruplicate, *P < 0.05 *vs* vehicle group. (**C**) Nude mice with pre-established U87MG orthotopic tumors received continuous brain infusions of vehicle (0.2 % DMSO), 0.1 mM of 5-HEAT, UCM799 or UCM1400. Mice were euthanized 14 days after treatment initiation for tumor volume evaluation. Values were normalized by the average tumor volume of all groups obtained on each of the five experimental days. Data are shown as mean ± SEM, **P < 0.001, ***P < 0.0001 according to independent "t" Student test.

approximately 70 %, a robust therapeutic effect comparable to that observed with 5-HEAT and UCM799 (*N*-(2-(benzyl(3-methoxyphenyl) amino)ethyl)acetamide, a *N*-anilinoethylamide derivative characterized by the same subtype-selective mixed agonist-antagonist behavior [16]) (Fig. 7C).

4. Conclusions

N-Acylaminoethyl-THQs proved to be a versatile class of melatonergic ligands, amenable to modulation of binding affinity and intrinsic activity and characterized by structure-activity relationships consistent with those observed for other series of ligands [8,46]. Formal closure of the *N*-anilinoethylamide structure into a THQ nucleus afforded compounds endowed with nanomolar binding affinity and moderate MT_2 receptor selectivity. Molecular modelling simulations allowed to characterize the role of the THQ scaffold and of substituents, with investigation of conformational and configurational aspects responsible for modulation of binding affinity.

Replacement of the methoxy group with a 2-hydroxyethoxy substituent afforded compound **4d** (UCM1400) having an MT_1 agonist-MT_2 antagonist profile and higher MT_1 and MT_2 binding affinities than those recorded for 5-HEAT. UCM1400 exhibited significant in vitro antiproliferative effects on glioma cell lines and reduced in vivo tumor growth, highlighting the clinical potential of subtype-selective modulators of melatonin receptors in brain cancer therapy.

5. Experimental section

5.1. Chemistry

5.1.1. General procedures

Melting points were determined on a Buchi B-540 capillary melting point apparatus and are uncorrected. ^{1}H NMR and ^{13}C NMR spectra were recorded on a Bruker AVANCE 200, 400, or Bruker Avance Neo Ascend 600, using $CDCl_3$ as solvent unless stated otherwise. Chemical shifts (δ scale) are reported in parts per million (ppm) relative to the central peak of the solvent; coupling constants (J) are given in hertz (Hz). ESI MS spectra were taken on a Waters Micromass ZQ instrument; molecular ions $[M+H]^+$ are given. High-resolution mass spectrometry (HRMS) analysis was performed on Orbitrap Exploris 240 Mass Spectrometer (Thermo Fisher Scientific), molecular ions $[M+H]^+$ are given. Optical rotation analysis was performed using a Perkin-Elmer 241 polarimeter using a sodium lamp (λ 589 nm, D-line), α values were determined at 20 °C and are reported in 10^{-1} deg cm^2 g^{-1}; concentration (c) is in g per 100 mL. Enantiomeric purity was determined by HPLC on the following apparatus: Shimadzu LC-10AT (liquid chromatograph), Shimadzu SPD-10A (UV detector), Shimadzu C–R6A Chromatopac (integrator). The purity of tested compounds, determined by HPLC, was greater than 95 %. These analyses were performed on a Waters HPLC/DAD/MS system (separation module Alliance HT2795, Photo Diode Array Detector 2996, mass detector Micromass ZQ; software: MassLynx 4.1) using Gemini® C6-Phenyl column (1500 mm × 4.6 mm i.d., 5-μm particle size). Linear gradient of 0.1 % formic acid aqueous solution and acetonitrile 40/60 to 100 % acetonitrile for 8 min then 100 % acetonitrile for 2 min. HPLC settings were as follows: flow rate, 1.0 mL/min; injection volume, 10.0 μL; detector wavelength, 254 nm. Column chromatography purifications were performed under "flash" conditions using Merck 230–400 mesh silica gel. Analytical thin-layer chromatography (TLC) was carried out on Merck silica gel 60 F_{254} plates. All commercially available starting materials and solvents are reagent grade and used without further purification.

5.1.1.1. General procedure for O-alkylation of 7-hydroxy-1,2,3,4-tetrahydroquinoline. NaH (60 % in mineral oil, 0.04 g, 1 mmol) was added to a stirred solution of 7-hydroxy-1,2,3,4-tetrahydroquinoline (163 mg, 1 mmol) in dry DMF (1.8 mL) at −10 °C under N_2 atmosphere. After 30 min the opportune alkyl halide (1 mmol) was added to the reaction mixture and the stirring continued at room temperature for a further 6 h. The mixture was poured into ice-cooled water and extracted with EtOAc. The combined organic phases were washed with brine, dried (Na_2SO_4), and evaporated to give a crude residue that was purified by flash chromatography.

*5.1.1.2. General procedure for reductive N-alkylation of derivatives **2a-g**.* TFA (1 mL) and TES (0.4 mL, 2.5 mmol) were added to a solution of the opportune tetrahydroquinoline intermediate **2a-g** (1 mmol) and appropriate acetal (1.4 mmol) in DCM (2 mL), and the resulting mixture was stirred at room temperature for 2 h under a nitrogen atmosphere. After cooling to 0 °C, the reaction mixture was carefully neutralized with an aqueous saturated solution of $NaHCO_3$ and diluted with DCM. The

aqueous phase was extracted with DCM and the combined organic phases were washed with brine and dried over Na_2SO_4. The solvent was removed by distillation, and the crude residue was purified by column chromatography.

*5.1.1.3. General procedure for the reduction of the carboxymethyl group of **3d-f**.* $LiAlH_4$ (0.08 g, 2.10 mmol) was added in small portions to an ice-cooled stirred solution of the opportune carboxymethyl derivative **3d-f** (1 mmol) in dry THF (12 mL) under N_2. Upon completion of the addition, the mixture was stirred at 0 °C for 1 h, then H_2O was carefully added to destroy the unreacted $LiAlH_4$, and the resulting mixture was filtered through a celite pad. The filtrate was concentrated *in vacuo*, and the residue was partitioned between H_2O and EtOAc. The combined organic phases were washed with brine, dried (Na_2SO_4), and evaporated to yield the crude desired product that was purified by flash chromatography.

*5.1.1.4. General procedure for hydrogenation of nitriles and concomitant N-acylation of **23a-b**.* A solution of the opportune nitrile derivative (0.23 mmol), in THF (12 mL) and propionic anhydride (0.28 mL, 2.2 mmol) was hydrogenated (4 atm) over Raney Nickel for 6 h at 60 °C. The catalyst was filtered on Celite, the filtrate was concentrated *in vacuo*, and the residue was partitioned between EtOAc and 2 N NaOH. The organic layer was washed with brine, dried (Na_2SO_4) and evaporated under reduced pressure to give a crude material of the desired product.

5.1.2. Compound synthesis and characterization

*5.1.2.1. 7-(2-Methoxyethoxy)-1,2,3,4-tetrahydroquinoline **(2b)**.* This product was prepared according to the above-described general procedure using 1-bromo-2-methoxyethane as alkylating agent. Flash chromatography: silica gel, DCM/EtOAc 9:1 as eluent. Oil, 70 % yield. ^{1}H NMR (400 MHz, $CDCl_3$) δ: 6.84 (d, 1H, J = 8.0 Hz), 6.22 (dd, 1H, J = 2.5 and 8.0 Hz), 6.08 (d, 1H, J = 2.5 Hz), 4.07–4.07 (m, 2H), 3.81 (brs, 1H), 3.73-3.71 (m, 2H), 3.44 (s, 3H), 3.29-3.26 (m, 2H), 2.70 (t, 2H, J = 6.5 Hz), 1.95-1.89 (m, 2H). ESI MS (m/z): 208 $[M+H]^+$.

*5.1.2.2. 7-(3-Fluoropropoxy)-1,2,3,4-tetrahydroquinoline **(2c)**.* This product was prepared according to the above-described general procedure using 1-fluoro-3-iodopropane as alkylating agent. Flash chromatography: silica gel, cyclohexane/EtOAc 7:3 as eluent. Oil, 63 % yield. ^{1}H NMR (400 MHz, $CDCl_3$) δ: 6.84 (d, 1H, J = 8.0 Hz), 6.20 (dd, 1H, J = 2.5 and 8.0 Hz), 6.05 (d, 1H, J = 2.5 Hz), 4.63 (dt, 2H, J = 6.0 and 47.0 Hz), 4.03 (t, 2H, J = 6.0 Hz), 3.83 (brs, 1H), 3.30-3.27 (m, 2H), 2.70 (t, 2H, J = 6.5 Hz), 2.20-2.07 (m, 2H), 1.95-1.89 (m, 2H). ESI MS (m/z): 210 $[M+H]^+$.

*5.1.2.3. Methyl 2-[(1,2,3,4-tetrahydroquinolin-7-yl)oxy]acetate **(2d)**.* This product was prepared according to the above-described general procedure using methyl chloroacetate as alkylating agent. Flash chromatography: silica gel, cyclohexane/EtOAc 7:3 as eluent. Oil, 62 % yield. ^{1}H NMR (400 MHz, $CDCl_3$) δ: 6.84 (d, 1H, J = 8.0 Hz), 6.17 (dd, 1H, J = 2.5 and 8.0 Hz), 6.06 (d, 1H, J = 2.5 Hz), 4.57 (s, 2H), 3.80 (s, 3H), 3.65 (brs, 1H), 3.28-3.25 (m, 2H), 2.69 (t, 2H, J = 6.5 Hz), 1.94-1.88 (m, 2H). ESI MS (m/z): 222 $[M+H]^+$.

*5.1.2.4. N-{2-[7-methoxy-3,4-dihydroquinolin-1(2H)-yl]ethyl}propionamide **(3a)**.* This product was prepared according to the above-described general procedure starting from **2a** and using *N*-(2,2-dimethoxyethyl) propionamide [21] as acetal. Flash chromatography: silica gel, cyclohexane/EtOAc 4:6 as eluent. White solid, mp 67-8 °C (diethyl ether-petroleum ether); 55 % yield. ^{1}H NMR (400 MHz, $CDCl_3$) δ: 6.86 (d, 1H, J = 8.0 Hz), 6.25 (d, 2H, J = 2.0 Hz), 6.19 (dd, 1H, J = 2.0 and 8.0 Hz), 5.65 (brs, 1H), 3.77 (s, 3H), 3.51-3.47 (m, 2H), 3.42-3.39 (m,2H), 3.28 (t, 2H, J = 5.5 Hz), 2.71 (t, 2H, J = 6.5 Hz), 2.19 (q, 2H, J = 7.5 Hz), 1.96-1.90 (m, 2H), 1.14 (t, 3H, J = 7.5 Hz). ^{13}C NMR (100 MHz, $CDCl_3$) δ: 174.0, 159.3, 146.1, 129.7, 115.2, 100.6, 97.4, 55.2, 50.6, 49.7, 36.7, 29.7, 27.3, 22.4, 9.7. ESI MS (m/z) 263 $[M+H]^+$. HPLC purity 100 % (t_R 3.03).

*5.1.2.5. N-{2-[7-(2-methoxyethoxy)-3,4-dihydroquinolin-1(2H)-yl]ethyl} propionamide **(3b)**.* This product was prepared according to the above-described general procedure starting from **2b** and using *N*-(2,2-dimethoxyethyl)propionamide [21] as acetal. Flash chromatography: silica gel, cyclohexane/EtOAc 3:7 as eluent. Beige solid, 40 % yield. ^{1}H NMR (400 MHz, $CDCl_3$) δ: 6.82 (d, 1H, J = 8.0 Hz), 6.25 (d, 1H, J = 2.5 Hz), 6.16 (dd, 1H, J = 2.5 and 8.0 Hz), 6.03 (brt, 1H), 4.08-4.06 (m, 2H), 3.72-3.70 (m, 2H), 3.47-3.41 (m, 2H), 3.42 (s, 3H), 3.38-3.34 (m, 2H), 3.25 (t, 2H, J = 5.5 Hz), 2.67 (t, 2H, J = 6.5 Hz), 2.19 (q, 2H, J = 7.5 Hz), 1.92-1.86 (m, 2H), 1.11 (t, 3H, J = 7.5 Hz). ^{13}C NMR (100 MHz, $CDCl_3$) δ: 174.6, 158.4, 145.8, 129.7, 115.7, 101.5, 98.5, 71.2, 67.1, 59.1, 50.6, 49.6, 36.7, 29.6, 27.2, 22.1, 9.7. ESI MS (m/z): 307 $[M+H]^+$. HPLC purity 100 % (t_R 2.93).

*5.1.2.6. N-{2-[7-(3-fluoropropoxy)-3,4-dihydroquinolin-1(2H)-yl]ethyl} propionamide **(3c)**.* This product was prepared according to the above-described general procedure starting from **2c** and using *N*-(2,2-dimethoxyethyl)propionamide [21] as acetal. Flash chromatography: silica gel, EtOAc/cyclohexane 7:3 as eluent. White solid, mp 87-8 °C (diethyl ether/petroleum ether); 39 % yield. ^{1}H NMR (400 MHz, $CDCl_3$) δ: 6.85 (d, 1H, J = 8.0 Hz), 6.23 (d, 1H, J = 2.5 Hz), 6.17 (dd, 1H, J = 2.5 and 8.0 Hz), 5.66 (brt, 1H), 4.64 (dt, 2H, J = 6.0 and 47.0 Hz), 4.07 (t, 2H, J = 6.0 Hz), 3.51-3.46 (m, 2H), 3.42-3.38 (m, 2H), 3.30-3.27 (m, 2H), 2.70 (t, 2H, J = 6.5 Hz), 2.22-2.09 (m, 4H), 1.96-1.90 (m, 2H), 1.14 (t, 3H, J = 7.5 Hz). ^{13}C NMR (100 MHz, $CDCl_3$) δ: 174.0, 158.5, 146.2, 129.8, 115.4, 101.2, 98.0, 81.0 (J = 163.0 Hz), 63.4, 50.6, 49.7, 36.8, 30.5 (J = 20 Hz), 29.7, 27.3, 22.4, 9.7. ESI MS (m/z): 309 $[M+H]^+$. HPLC purity 98.5 % (t_R 3.40).

*5.1.2.7. Methyl 2-{[1-(2-propionamidoethyl)-1,2,3,4-tetrahydroquinolin-7-yl]oxy}acetate **(3d)**.* This product was prepared according to the above-described general procedure starting from **2d** and using *N*-(2,2-dimethoxyethyl)propionamide [21] as acetal. Flash chromatography: silica gel, gradient from cyclohexane/EtOAc 3:7 to EtOAc. Oil, 62 % yield. ^{1}H NMR (400 MHz, $CDCl_3$) δ: 6.82 (d, 1H, J = 8.0 Hz), 6.25 (d, 1H, J = 2.5 Hz), 6.09 (brt, 1H), 6.06 (dd, 1H, J = 2.5 and 8.0 Hz), 4.58 (s, 2H), 3.79 (s, 3H), 3.45-3.40 (m, 2H), 3.37-3.34 (m, 2H), 3.27 (t, 2H, J = 5.5 Hz), 2.66 (t, 2H, J = 6.5 Hz), 2.19 (q, 2H, J = 7.5 Hz), 1.92-1.86 (m, 2H), 1.13 (t, 3H, J = 7.5 Hz). ESI MS (m/z): 321 $[M+H]^+$.

*5.1.2.8. Methyl 2-{[1-(2-acetamidoethyl)-1,2,3,4-tetrahydroquinolin-7-yl]oxy}acetate **(3e)**.* This product was prepared according to the above-described general procedure starting from **2d** and using *N*-(2,2-dimethoxyethyl)acetamide [22] as acetal. Flash chromatography: silica gel, cyclohexane/EtOAc 3:7 as eluent. Oil, 57 % yield. ^{1}H NMR (400 MHz, $CDCl_3$) δ: 6.84 (d, 1H, J = 8.0 Hz), 6.29 (d, 1H, J = 2.5 Hz), 6.10 (dd, 1H, J = 2.5 and 8.0 Hz), 5.74 (brs, 1H), 4.61 (s, 2H), 3.80 (s, 3H), 3.48-3.43 (m, 2H), 3.40-3.37 (m, 2H), 3.28 (t, 2H, J = 5.5 Hz), 2.69 (t, 2H, J = 6.5 Hz), 1.97 (s, 3H), 1.96-1.88 (m, 2H). ESI MS (m/z): 307 $[M+H]^+$.

*5.1.2.9. Methyl 2-{[1-(2-(2,2-difluoroacetamido)ethyl)-1,2,3,4-tetrahydroquinolin-7-yl]oxy}acetate **(3f)**.* Methyl difluoroacetate (0.38 mL, 4.32 mmol) was added to a solution of 2,2-dimethoxyethanamine (0.52 mL, 4.8 mmol) in acetonitrile (4.8 mL) and the mixture was stirred at room temperature for 48 h. After evaporation of volatiles under vacuum the crude residue was purified by flash chromatography (DCM/MeOH 99:1 as eluent) to afford pure *N*-(2,2-dimethoxyethyl)-2,2-difluoroacetamide as an oil; yield 85 %. ^{1}H NMR (400 MHz, $CDCl_3$) δ: 6.70 (brs, 1H), 5.89 (t, 1H, J = 53.0 Hz), 4.40 (t, 1H, J = 5.5 Hz), 3.42 (m, 2H), 3.37 (s, 6H). This acetal was used for the synthesis of **3f** that was

accomplished according to the general procedure of reductive *N*-alkylation above-described starting from **2d**. Flash chromatography: silica gel, cyclohexane/EtOAc 7:3 as eluent. Oil, 43 % yield. ^{1}H NMR (400 MHz, $CDCl_3$) δ: 6.87 (d, 1H, $J = 8.0$ Hz), 6.54 (brs, 1H), 6.28 (d, 1H, $J = 2.5$ Hz), 6.14 (dd, 1H, $J = 2.5$ and 8.0 Hz), 5.89 (t, 1H, $J = 54.0$ Hz), 4.61 (s, 2H), 3.80 (s, 3H), 3.60-3.55 (m, 2H), 3.48-3.43 (m, 2H), 3.29 (t, 2H, $J = 5.5$ Hz), 2.70 (t, 2H, $J = 6.5$ Hz), 1.96-1.90 (m, 2H). ESI MS (*m/z*): 343 $[M+H]^+$.

*5.1.2.10. N-[2-(7-methoxy-3,4-dihydroquinolin-1(2H)-yl)ethyl]acetamide (**3g**).* This product was prepared according to the above-described general procedure starting from **2a** and using *N*-(2,2-dimethoxyethyl)acetamide [22] as acetal. Flash chromatography: silica gel, EtOAc/cyclohexane 7:3 as eluent. Beige solid, mp 80-1 °C (diethyl ether/petroleum ether); 48 % yield. ^{1}H NMR (400 MHz, $CDCl_3$) δ: 6.87 (d, 1H, $J = 8.0$ Hz), 6.25 (d, 1H, $J = 2.5$ Hz), 6.18 (dd, 1H, $J = 2.5$ and 8.0 Hz), 5.65 (brs, 1H), 3.78 (s, 3H), 3.49-3.45 (m, 2H), 3.42-3.38 (m, 2H), 3.29 (t, 2H, $J = 5.5$ Hz), 2.70 (t, 2H, $J = 6.5$ Hz), 1.97 (s, 3H), 1.96-1.90 (m, 2H). ^{13}C NMR (150 MHz, $CDCl_3$) δ: 170.4, 159.3, 145.9, 129.8, 115.5, 101.0, 97.7, 55.3, 50.9, 49.6, 36.8, 27.2, 23.3, 22.2. ESI MS (*m/z*): 249 $[M+H]^+$. HPLC purity 100 % (t_R 2.72). HRMS (ESI): *m/z* calculated for $C_{14}H_{21}N_2O_2$, $[M+H]^+$ 249.1603; found 249.1598.

*5.1.2.11. N-{2-[7-(2-hydroxyethoxy)-3,4-dihydroquinolin-1(2H)-yl]ethyl}propionamide (**4d**).* This product was prepared following the above-described general procedure starting from **3d**. Flash chromatography: silica gel, EtOAc as eluent. Amorphous solid, 88 % yield. ^{1}H NMR (400 MHz, $CDCl_3$) δ: 6.85 (d, 1H, $J = 8.0$ Hz), 6.38 (d, 1H, $J = 2.5$ Hz), 6.17 (dd, 1H, $J = 2.5$ and 8.0 Hz), 5.69 (brs, 1H), 4.12-4.09 (m, 2H), 3.95-3.91 (m, 2H), 3.49-3.44 (m, 2H), 3.41-3.37 (m, 2H), 3.30-3.27 (m, 2H), 2.70 (t, 2H, $J = 6.5$ Hz), 2.55 (brt, 1H), 2.21 (q, 2H, $J = 7.5$ Hz), 1.96-1.90 (m, 2H), 1.15 (t, 3H, $J = 7.5$ Hz). ^{13}C NMR (100 MHz, $CDCl_3$) δ: 174.3, 158.4, 146.1, 129.7, 115.4, 101.8, 97.8, 69.1, 61.3, 50.6, 49.7, 36.6, 29.6, 27.3, 22.4. ESI MS (*m/z*): 293 $[M+H]^+$. HPLC purity 100 % (t_R 2.37). HRMS (ESI): *m/z* calculated for $C_{16}H_{25}N_2O_3$, $[M+H]^+$ 293.1865; found 293.1862.

*5.1.2.12. N-{2-[7-(2-hydroxyethoxy-3,4-dihydroquinolin-1(2H)-yl]ethyl}acetamide (**4e**).* This product was prepared following the above-described general procedure starting from **3e**. Flash chromatography: silica gel, EtOAc as eluent. Amorphous solid; 83 % yield. ^{1}H NMR (400 MHz, $CDCl_3$) δ: 6.85 (d, 1H, $J = 8.0$ Hz), 6.39 (d, 1H, $J = 2.5$ Hz), 6.19 (dd, 1H, $J = 2.5$ and 8.0 Hz), 5.98 (brs, 1H), 4.10-4.08 (m, 2H), 3.94-3.91 (m, 2H), 3.47-3.36 (m, 4H), 3.29 (t, 2H, $J = 5.5$ Hz), 2.70 (t, 2H, $J = 6.5$ Hz), 1.99 (s, 3H), 1.97-1.90 (m, 2H). ^{13}C NMR (100 MHz, $CDCl_3$) δ: 170.8, 158.4, 145.7, 129.8, 115.6, 102.4, 98.3, 69.2, 61.3, 50.9, 49.6, 36.6, 27.1, 23.2, 22.1. ESI MS (*m/z*): 279 $[M+H]^+$. HPLC purity 100 % (t_R 2.22).

*5.1.2.13. 2,2-Difluoro-N-{2-[7-(2-hydroxyethoxy)-3,4-dihydroquinolin-1(2H)-yl]ethyl}acetamide (**4f**).* This product was prepared following the above-described general procedure starting from **3f**. Flash chromatography: silica gel, cyclohexane/EtOAc 3:7 as eluent. Yellow solid, 54 % yield. ^{1}H NMR (400 MHz, $CDCl_3$) δ: 6.87 (d, 1H, $J = 8.0$ Hz), 6.56 (brs, 1H), 6.28 (d, 1H, $J = 2.5$ Hz), 6.20 (dd, 1H, $J = 2.5$ and 8.0 Hz), 5.89 (t, 1H, $J = 54.0$ Hz), 4.09-4.07 (m, 2H), 3.95-3.93 (m, 2H), 3.60-3.55 (m, 2H), 3.47-3.43 (m, 2H), 3.29 (t, 2H, $J = 5.5$ Hz), 2.71 (t, 2H, $J = 6.5$ Hz), 2.13 (brt, 1H), 1.97-1.91 (m, 2H). ^{13}C NMR (100 MHz, $CDCl_3$) δ: 163.1 (t, $J = 24.5$ Hz), 158.3, 145.7, 129.9, 115.8, 108.4 (t, $J = 250.5$ Hz), 101.8, 98.1, 69.2, 61.4, 50.1, 49.9, 36.4, 27.2, 22.3. ESI MS (*m/z*): 315 $[M+H]^+$. HPLC purity 95.4 % (t_R 2.72).

*5.1.2.14. 2-{[1-(2-Acetamidoethyl)-1,2,3,4-tetrahydroquinolin-7-yl]oxy}propionamide (**5**).* A solution of methyl 2-{[1-(2-propionamidoethyl)-1,2,3,4-tetrahydroquinolin-7-yl]oxy}acetate **3d** (160 mg, 0.5 mmol) in 2 M NH_3 in EtOH (12.8 mmol, 6.4 mL) was stirred at room temperature for 24 h. The solvent was evaporated under reduced pressure and the oily residue was purified by flash chromatography (EtOAc/MeOH 3 % as eluent) and crystallization. White solid, mp 165–7 °C (EtOAc); 64 % yield. ^{1}H NMR (600 MHz, DMSO-d_6) δ: 7.88 (brt, 1H), 7.36 (brd, 2H), 6.75 (d, 1H, $J = 8.0$ Hz), 6.28 (d, 1H, $J = 2.5$ Hz), 6.06 (dd, 1H, $J = 2.5$ and 8.0 Hz), 4.33 (s, 2H), 3.27-3.19 (m, 6H), 2.59 (t, 2H, $J = 6.5$ Hz), 2.06 (q, 2H, $J = 7.5$ Hz), 1.82-1.78 (m, 2H), 0.98 (t, 3H, $J = 7.5$ Hz). ^{13}C NMR (150 MHz, DMSO-d_6): δ 173.6, 170.8, 157.8, 146.1, 129.6, 115.4, 101.4, 98.0, 67.3, 50.3, 49.4, 35.8, 29.0, 27.3, 22.3, 10.3. ESI MS (*m/z*): 306 $[M+H]^+$. HPLC purity 96.4 % (t_R 2.23).

*5.1.2.15. N-{2-[7-hydroxy-3,4-dihydroquinolin-1(2H)-yl]ethyl}propionamide (**6**).* A solution of 1 M BBr3 in DCM (0.9 mL, 0.9 mmol) in dry DCM (3.5 mL) was added dropwise at 0 °C to a solution of *N*-{2-[7-methoxy-3,4-dihydroquinolin-1(2*H*)-yl]ethyl}propionamide **3a** (120 mg, 0.46 mmol) in dry DCM (3.5 mL) stirred under nitrogen atmosphere. The resulting mixture was stirred 20 h at room temperature, quenched by adding an aqueous saturated solution of $NaHCO_3$ until neutral pH and then extracted with DCM. The organic phases were combined, washed with brine, dried (Na_2SO_4) and concentrated under reduced pressure to give a crude material which was purified by flash chromatography over silica gel (cyclohexane/EtOAc 2:8 as eluent). Yellowish solid, mp 119-20 °C (EtOAc-petroleum ether); 74 % yield. ^{1}H NMR (200 MHz, $CDCl_3$) δ: 6.80 (d, 1H, $J = 8.0$ Hz), 6.27 (d, 2H, $J = 2.5$ Hz), 6.13 (dd, 1H, $J = 2.5$ and 8.0 Hz), 5.78 (brs, 1H), 3.48-3.39 (m, 4H), 3.29-3.25 (m, 2H), 2.68 (t, 2H, $J = 6.0$ Hz), 2.23 (q, 2H, $J = 7.5$ Hz), 1.95-1.91 (m, 2H), 1.16 (t, 3H, $J = 7.5$ Hz). ESI MS (*m/z*) 249 $[M+H]^+$.

*5.1.2.16. N-{2-[7-(4-phenylbuthoxy)-3,4-dihydroquinolin-1(2H)-yl]ethyl}propionamide (**7**).* NaH (80 % in mineral oil, 9 mg, 0.3 mmol) and 1-bromo-4-phenylbutane (98 mg, 81 μl, 0.46 mmol) were added at −10 °C under nitrogen to a solution of *N*-{2-[7-hydroxy-3,4-dihydroquinolin-1(2*H*)-yl]ethyl}propionamide **6** (70 mg, 0.28 mmol) in dry DMF (2 mL). The reaction mixture was stirred 6 h at room temperature, quenched by adding water and then extracted with EtOAc. The organic phases were combined, washed with brine, dried (Na_2SO_4) and concentrated under reduced pressure to give a crude material which was purified by flash chromatography over silica gel (cyclohexane/EtOAc 2:8 as eluent). White solid, mp 82-3 °C (diethyl ether-petroleum ether); 92 % yield. ^{1}H NMR (400 MHz, $CDCl_3$) δ: 7.17–7.31 (m, 5H), 6.84 (d, 1H, $J = 8.0$ Hz), 6.21 (d, 2H, $J = 2.5$ Hz), 6.15 (dd, 1H, $J = 2.5$ and 8.0 Hz), 5.62 (brs, 1H), 3.95-3.92 (m, 2H), 3.50-3.45 (m, 2H), 3.41-3.38 (m, 2H), 3.29-3.26 (m, 2H), 2.71-2.67 (m, 4H), 2.18 (q, 2H, $J = 7.5$ Hz), 1.95-1.89 (m, 2H), 1.82-1.78 (m, 4H), 1.13 (t, 3H, $J = 7.5$ Hz). ^{13}C NMR (50 MHz, $CDCl_3$) δ: 173.9, 158.7, 146.1, 142.3, 129.7, 128.4, 128.3, 125.7, 115.2, 101.1, 98.1, 67.6, 50.6, 49.7, 36.8, 35.6, 29.7, 29.0, 27.9, 27.3, 22.4, 9.7. ESI MS (*m/z*) 381 $[M+H]^+$. HPLC purity 97.6 % (t_R 5.54).

*5.1.2.17. N-[2-(6-methoxy-2,3-dihydro-4H-benzo[b][1,4]oxazin-4-yl)ethyl]propionamide (**8**).* This product was prepared according to the above-described general procedure for reductive *N*-alkylation starting from commercially available 6-methoxy-3,4-dihydro-2*H*-benzo[*b*][1,4]oxazine and using *N*-(2,2-dimethoxyethyl)propionamide [21] as acetal. Flash chromatography: silica gel, cyclohexane/EtOAc 3:7 as eluent. White solid, mp 104-5 °C (diethyl ether/petroleum ether); 29 % yield. ^{1}H NMR (400 MHz, $CDCl_3$) δ: 6.71 (d, 1H, $J = 8.5$ Hz), 6.33 (d, 1H, $J = 3.0$ Hz), 6.18 (dd, 1H, $J = 3.0$ and 8.5 Hz), 5.74 (brs, 1H), 4.19-4.16 (m, 2H), 3.75 (s, 3H), 3.52-3.47 (m, 2H), 3.42-3.36 (m, 4H), 2.19 (q, 2H, $J = 7.5$ Hz), 1.14 (t, 3H, $J = 7.5$ Hz). ^{13}C NMR (100 MHz, $CDCl_3$) δ: 174.1, 154.8, 138.3, 135.2, 116.6, 101.8, 99.2, 64.0, 55.6, 50.4, 47.5, 36.6, 29.7, 9.7. ESI MS (*m/z*): 265 $[M+H]^+$. HPLC purity 100 % (t_R 2.72).

*5.1.2.18. Methyl 2-[(3,4-dihydro-2H-benzo[b][1,4]oxazin-6-yl)oxy]acetate (**9**).* This product was prepared according to the above-described general procedure of *O*-alkylation starting from commercially available 3,4-dihydro-2*H*-benzo[*b*][1,4]oxazin-6-ol and using methyl chloroacetate as alkylating agent. Flash chromatography: silica gel, cyclohexane/EtOAc 1:1 as eluent. Oil, 73 % yield. ^{1}H NMR (400 MHz, $CDCl_3$) δ: 6.68 (d, 1H, J = 8.5 Hz), 6.21 (dd, 1H, J = 3.0 and 8.5 Hz), 6.18 (d, 1H, J = 3.0 Hz), 4.55 (s, 2H), 4.22-4.20 (m, 2H), 3.82 (brs, 1H), 3.80 (s, 3H), 3.42-3.40 (m, 2H). ESI MS (*m/z*): 224 $[M+H]^+$.

*5.1.2.19. Methyl 2-{[4-(2-propionamidoethyl)-3,4-dihydro-2H-benzo[b][1,4]oxazin-6-yl]oxy}acetate (**10**).* This product was prepared according to the above-described general procedure for reductive *N*-alkylation starting from **9** and using *N*-(2,2-dimethoxyethyl)propionamide [21] as acetal. Flash chromatography: silica gel, EtOAc as eluent. Amorphous solid, 52 % yield. ^{1}H NMR (400 MHz, $CDCl_3$) δ: 6.68 (d, 1H, J = 8.5 Hz), 6.39 (d, 1H, J = 3.0 Hz), 6.10 (dd, 1H, J = 3.0 and 8.5 Hz), 5.74 (brt, 1H), 4.57 (s, 2H), 4.17-4.15 (m, 2H), 3.80 (s, 3H), 3.50-3.45 (m, 2H), 3.41-3.36 (m, 4H), 2.19 (q, 2H, J = 7.5 Hz), 1.14 (t, 3H, J = 7.5 Hz). ESI MS (*m/z*): 323 $[M+H]^+$.

*5.1.2.20. N-{2-[6-(2-hydroxyethoxy)-2,3-dihydro-4H-benzo[b][1,4]oxazin-4-yl]ethyl}propionamide (**11**).* This product was prepared following the above-described general procedure of reduction of the carboxymethyl group starting from **10**. Flash chromatography: silica gel, EtOAc as eluent. Oil; 64 % yield. ^{1}H NMR (400 MHz, $CDCl_3$) δ: 6.69 (d, 1H, J = 8.5 Hz), 6.45 (d, 1H, J = 3.0 Hz), 6.18 (dd, 1H, J = 3.0 and 8.5 Hz), 5.69 (brs, 1H), 4.19-4.17 (m, 2H), 4.07-4.05 (m, 2H), 3.94-3.90 (m, 2H), 3.50-3.36 (m, 6H), 2.45 (brt, 1H), 2.21 (q, 2H, J = 7.5 Hz), 1.15 (t, 3H, J = 7.5 Hz). ^{13}C NMR (100 MHz, $CDCl_3$) δ: 174.4, 153.9, 138.4, 135.5, 116.5, 102.7, 99.6, 69.7, 64.2, 61.4, 50.1, 47.5, 36.6, 29.6, 9.7. ESI MS (*m/z*): 295 $[M+H]^+$. HPLC purity 98.8 % (t_R 2.29).

*5.1.2.21. Methyl 2-{[8-(2-acetamidoethyl)naphthalen-2-yl]oxy}acetate (**12**).* This product was prepared following the above-described general procedure of *O*-alkylation starting from *N*-[2-(7-hydroxynaphtalen-1-yl) ethyl]acetamide [23] and using methyl chloroacetate as alkylating agent. Flash chromatography: silica gel, EtOAc as eluent. Amorphous solid; 76 % yield. ^{1}H NMR (400 MHz, $CDCl_3$) δ: 7.80 (d, 1H, J = 9.0 Hz), 7.72-7.69 (m, 1H), 7.46 (d, 1H, J = 2.5 Hz), 7.32-7.29 (m, 2H), 7.25 (dd, 1H, J = 2.5 and 9.0 Hz), 4.85 (s, 2H), 3.84 (s, 3H), 3.61-3.56 (m, 2H), 3.23 (t, 2H, J = 7.0 Hz), 1.98 (s, 3H). ESI MS (*m/z*): 302 $[M+H]^+$.

*5.1.2.22. N-{2-[7-(2-hydroxyethoxy)naphthalen-1-yl]ethyl}acetamide (**13**).* This product was prepared following the above-described general procedure of reduction of the carboxymethyl group starting from **12**. Flash chromatography: silica gel, EtOAc-5 % MeOH as eluent. Off-white solid, 77 % yield. ^{1}H NMR (400 MHz, $CDCl_3$) δ: 7.76 (d, 1H, J = 9.0 Hz), 7.69-7.67 (m, 2H), 7.30-7.24 (m, 2H), 7.18 (dd, 1H, J = 2.5 and 9.0 Hz), 6.03 (brs, 1H), 4.36 (t, 2H, J = 5.5 Hz), 4.04 (t, 2H, J = 5.5 Hz), 3.60-3.55 (m, 2H), 3.27-3.22 (m, 2H), 2.83 (brs, 1H), 2.02 (s, 3H). ^{13}C NMR (100 MHz, $CDCl_3$) δ: 170.9, 157.1, 133.4, 133.2, 130.3, 129.4, 127.2, 127.1, 123.2, 118.7, 103.5, 69.1, 60.8, 40.6, 33.7, 23.3. ESI MS (*m/z*): 274 $[M+H]^+$. HPLC purity 100 % (t_R 2.47).

*5.1.2.23. S-(2-{[1-(2-propionamidoethyl)-1,2,3,4-tetrahydroquinolin-7-yl]oxy}ethyl) ethanethioate (**14**).* A solution of $P(Ph)_3$ (59 mg, 0.22 mmol) and DIAD (46 mg, 0.22 mmol) in dry THF (0.55 mL) was stirred at 0 °C for 30 min. To this mixture, a solution of **4d** (42 mg, 0.14 mmol) and thioacetic acid (17 mg, 0.22 mmol) in dry THF (0.2 mL) was added at 0 °C and the stirring continued at room temperature for 18 h. The reaction was quenched by the addition of a saturated solution of NH_4Cl and then extracted with EtOAc. The combined organic phases were dried over Na_2SO_4, the solvent removed by distillation and the crude residue purified by flash chromatography (cyclohexane/EtOAc 6:4 as eluent). Amorphous solid, 83 % yield. ^{1}H NMR (400 MHz, $CDCl_3$) δ: 6.83 (d, 1H, J = 8.0 Hz), 6.29 (d, 1H, J = 2.5 Hz), 6.14 (dd, 1H, J = 2.5 and 8.0 Hz), 5.81 (brs, 1H), 4.08-4.05 (m, 2H), 3.49-3.47 (m, 2H), 3.45-3.42 (m, 2H), 3.40-3.28 (m, 2H), 3.23 (t, 2H, J = 7.0 Hz), 2.70-2.67 (m, 2H), 2.37 (s, 3H), 2.19 (q, 2H, J = 7.5 Hz), 1.94-1.91 (m, 2H), 1.14 (t, 3H, J = 7.5 Hz).

*5.1.2.24. Bis(2-{[1-(2-propionamidoethyl)-1,2,3,4-tetrahydroquinolin-7-yl]oxy}ethyl)disulfide (**15**).* Sodium methoxide (10 mg, 0.18 mmol) was added to a solution of **14** (42 mg, 0.12 mmol) in dry MeOH (0.24 mL) and the resulting mixture was stirred at room temperature for 16 h. The reaction was quenched by addition of 2 N HCl and then extracted with DCM. The combined organic phases were dried over Na_2SO_4 and the solvent removed by distillation. The crude residue was purified by flash chromatography (EtOAc as eluent). Amorphous solid, 65 % yield. ^{1}H NMR (400 MHz, $CDCl_3$) δ: 6.83 (d, 2H, J = 8.0 Hz), 6.22 (d, 2H, J = 2.5 Hz), 6.16 (dd, 2H, J = 2.5 and 8.0 Hz), 5.88 (brt, 2H), 4.23-4.20 (m, 4H), 3.47-3.43 (m, 4H), 3.42-3.35 (m, 4H), 3.29-3.27 (m, 4H), 3.09-3.06 (m, 4H), 2.69 (t, 4H, J = 6.5 Hz), 2.19 (q, 4H, J = 7.5 Hz), 1.94-1.91 (m, 4H), 1.13 (t, 6H, J = 7.5 Hz).

*5.1.2.25. N-{2-[7-(2-mercaptoethoxy)-3,4-dihydroquinolin-1(2H)-yl]ethyl}propionamide (**16**).* To a solution of **15** (24 mg, 0.04 mmol) and TCEP (12 mg, 0.041 mmol) in dry MeOH (0.3 mL) was added acetate buffer (pH = 4.76, 70 μL) and the resulting mixture was stirred at 45 °C for 4 h. The reaction was quenched with water and extracted with DCM and EtOAc. The combined organic phases were dried over Na_2SO_4 and the solvent removed by distillation. Orange solid, 81 % yield. ^{1}H NMR (400 MHz, $CDCl_3$) δ: 6.83 (d, 1H, J = 8.0 Hz), 6.24 (d, 1H, J = 2.5 Hz), 6.13 (dd, 1H, J = 2.5 and 8.0 Hz), 5.72 (brt, 1H), 4.09-4.06 (m, 2H), 3.48-3.43 (m, 2H), 3.40-3.36 (m, 2H), 3.28-3.25 (m, 2H), 2.88-2.83 (m, 2H), 2.68 (t, 2H, J = 6.5 Hz), 2.18 (q, 2H, J = 7.5 Hz), 1.94-1.88 (m, 2H), 1.71-1.67 (m, 1H, J = 8.5 Hz), 1.13 (t, 3H, J = 7.5 Hz). ^{13}C NMR (100 MHz, $CDCl_3$) δ: 174.0, 158.1, 146.2, 129.7, 115.6, 101.3, 98.1, 69.5, 50.5, 49.6, 36.7, 29.7, 27.3, 24.0, 22.3, 9.8. ESI MS (*m/z*): 309 $[M+H]^+$. HPLC purity 100 % (t_R 3.67).

*5.1.2.26. (R,S)-4-(4-methoxy-2-nitrophenyl)but-3-yn-2-ol [(R,S)-**17a**].* CuI (20 mg, 0.1 mmol), $PdCl_2(PPh_3)_2$ (65 mg, 0.093 mmol) and (*R,S*)-but-3-yn-2-ol (280 μl, 3.6 mmol) were added to a solution of 1-iodo-4-methoxy-2-nitrobenzene (500 mg, 1.8 mmol) in dry Et_3N (4.5 mL). The resulting mixture was stirred under nitrogen atmosphere at 60 °C for 40 min, then it was quenched by adding water and extracted with EtOAc. The organic phases were combined, washed with brine, dried (Na_2SO_4) and concentrated under reduced pressure to give a crude material which was purified by flash chromatography over silica gel (DCM/EtOAc 95:5 as eluent). Beige solid, 88 % yield. ^{1}H NMR (200 MHz, $CDCl_3$) δ: 7.52 (d, 1H, J = 8.5 Hz), 7.55 (d, 1H, J = 2.5 Hz), 7.15 (dd, 1H, J = 2.5 and 8.5 Hz), 4.81 (q, 1H, J = 6.5 Hz), 3.90 (s, 3H), 1.90 (brs, 1H), 1.59 (d, 3H, J = 6.5 Hz). ESI MS (*m/z*) 239 $[M + NH_4]^+$.

*5.1.2.27. (R)-4-(4-methoxy-2-nitrophenyl)but-3-yn-2-ol [(R)-**17a**].* This product was obtained starting from (*R*)-but-3-yn-2-ol according to the procedure above described. Beige solid, mp 65-6 °C (diethyl ether-petroleum ether); 87 % yield. ^{1}H NMR and ESI MS data were in agreement with those reported for the racemate (*R,S*)-**17a**.

*5.1.2.28. (S)-4-(4-methoxy-2-nitrophenyl)but-3-yn-2-ol [(S)-**17a**].* This product was obtained starting from (*S*)-but-3-yn-2-ol according to the procedure above described. Beige solid, mp 66-7 °C (diethyl ether-petroleum ether); 70 % yield. ^{1}H NMR and ESI MS data were in agreement with those reported for the racemate (*R,S*)-**17a**.

*5.1.2.29. (R,S)-4-(2-amino-4-methoxyphenyl)butan-2-ol [(R,S)-**18a**].* A solution of alcohol (*R,S*)-**17a** (485 mg, 2.2 mmol), in absolute EtOH (35 mL) was hydrogenated (5 atm) over Pd/C 10 % (110 mg) for 24 h at

room temperature. The catalyst was filtered on Celite, the filtrate was concentrated *in vacuo*, and the residue was purified by flash chromatography over silica gel (cyclohexane/EtOAc 6:4 as eluent). Yellow solid, mp 56-7 °C (diethyl ether-petroleum ether); 93 % yield. ^{1}H NMR (200 MHz, $CDCl_3$) δ: 6.96 (d, 1H, J = 8.0 Hz), 6.33 (dd, 1H, J = 2.0 and 8.0 Hz), 6.28 (d, 1H, J = 2.0 Hz), 3.85-3.75 (m, 1H), 3.76 (s, 3H), 2.63-2.55 (m, 2H), 1.76-1.66 (m, 2H), 1.23 (d, 3H, J = 6.0 Hz). ESI MS (m/z) 196 $[M+H]^+$.

*5.1.2.30. (R)-4-(2-amino-4-methoxyphenyl)butan-2-ol [(R)-**18a**].* This product was obtained starting from (*R*)-**17a** according to the procedure above described. Beige solid, mp 70-1 °C (diethyl ether-petroleum ether); 72 % yield. ^{1}H NMR and ESI MS data were in agreement with those reported for the racemate (*R*,*S*)-**18a**.

*5.1.2.31. (S)-4-(2-amino-4-methoxyphenyl)butan-2-ol [(S)-**18a**].* This product was obtained starting from (*S*)-**17a** according to the procedure above described. Beige solid, mp 69–70 °C (diethyl ether-petroleum ether); 66 % yield. ^{1}H NMR and ESI MS data were in agreement with those reported for the racemate (*R*,*S*)-**18a**.

*5.1.2.32. (R,S)-4-[4-methoxy-2-(2,2,2-trifluoroacetamido)phenyl]butan-2-yl 2,2,2-trifluoroacetate [(R,S)-**19a**] and (R,S)-2,2,2-trifluoro-N-[2-(3-hydroxybutyl)-5-methoxyphenyl]acetamide [(R,S)-**20a**].* Et_3N (182 µl, 1.3 mmol) and trifluoroacetic anhydride (156 µl, 1.12 mmol) were added under nitrogen at 0 °C to a solution of (*R*,*S*)-**18a** (220 mg, 1.13 mmol) in dry DCM (6.5 mL). The resulting mixture was stirred for 15 min, then it was quenched by adding water and extracted with EtOAc. The organic phases were combined, washed with brine, dried (Na_2SO_4) and concentrated under reduced pressure to give a crude material which was purified by flash chromatography over silica gel (DCM/EtOAc 98:2 as eluent).

(*R*,*S*)-**19a:** oil; 30 % yield. ^{1}H NMR (200 MHz, $CDCl_3$) δ: 7.75 (brs, 1H), 7.29 (d, 1H, J = 2.5 Hz), 7.14 (d, 1H, J = 8.5 Hz), 6.83 (dd, 1H, J = 2.5 and 8.5 Hz), 5.19-5.07 (m, 1H), 3.82 (s, 3H), 2.65-2.49 (m, 2H), 2.01-1.86 (m, 2H), 1.41 (d, 3H, J = 6.5 Hz). ESI MS (m/z) 405 $[M + NH_4]^+$.

(*R*,*S*)-**20a**: oil; 55 % yield. ^{1}H NMR (200 MHz, $CDCl_3$) δ: 10.16 (brs, 1H), 7.46 (d, 1H, J = 2.5 Hz), 7.12 (d, 1H, J = 8.5 Hz), 6.78 (dd, 1H, J = 2.5 and 8.5 Hz), 3.82 (s, 3H), 3.57 (brs, 1H), 2.90-2.59 (m, 2H), 1.79-1.70 (m, 2H), 1.24 (d, 3H, J = 6.0 Hz). ESI MS (m/z) 292 $[M+H]^+$.

*5.1.2.33. (R)-2,2,2-trifluoro-N-[2-(3-hydroxybutyl)-5-methoxyphenyl] acetamide [(R)-**20a**] and (S)-2,2,2-trifluoro-N-[2-(3-hydroxybutyl)-5-methoxyphenyl]acetamide [(S)-**20a**].* These products were obtained starting from (*R*) or (*S*)-**18a** according to the procedure above described for (*R*,*S*)-**20a**. ^{1}H NMR and ESI MS data were in agreement with those reported for the racemate.

*5.1.2.34. Conversion of (R,S)-, (R)- or (S)-**19a** into (R,S)-, (R)- or (S)-**20a**.* NaH (60 % in mineral oil, 120 mg, 3 mmol) was added to a solution of (*R*,*S*)-, (*R*)- or (*S*)-**19a** (580 mg, 1.5 mmol) in dry DMF (7 mL) at 0 °C under nitrogen. The reaction mixture was stirred at room temperature for 3 h then it was quenched by adding water and extracted with EtOAc. The organic phases were combined, washed with brine, dried (Na_2SO_4) and concentrated under reduced pressure to give a crude material which was purified by flash chromatography over silica gel (cyclohexane/EtOAc 8:2 as eluent). ^{1}H NMR and ESI MS data of the product were in agreement to those reported for the corresponding (*R*, *S*)-, (*R*)- or (*S*)-alcohols **20a**, 85–90 % yield.

*5.1.2.35. (R,S)-4-[4-methoxy-2-(2,2,2-trifluoroacetamido)phenyl]butan-2-yl-methanesulfonate [(R,S)-**21a**].* Mesyl chloride (233 µl, 3 mmol) and pyridine (233 µl, 2.9 mmol) were added under nitrogen atmosphere at 0 °C to a solution of (*R*,*S*)-**20a** (220 mg, 0.76 mmol) in dry DCM (3.5 mL). The resulting mixture was stirred at room temperature overnight, then it was quenched by adding water and extracted with EtOAc. The organic phases were combined, washed with brine, dried (Na_2SO_4) and concentrated under reduced pressure to give a crude material which was purified by flash chromatography over silica gel (cyclohexane/EtOAc 6:4 as eluent). White solid, mp 70-1 °C (diethyl ether-petroleum ether); 79 % yield. ^{1}H NMR (200 MHz, $CDCl_3$) δ: 8.23 (brs,1H), 7.20 (d, 1H, J = 2.5 Hz), 7.21 (d, 1H, J = 8.5 Hz), 6.85 (dd, 1H, J = 2.5 and 8.5 Hz), 4.87-4.78 (m, 1H), 3.82 (s, 3H), 3.04 (s, 3H), 2.73-2.65 (m, 2H), 2.02-1.91 (m, 2H), 1.46 (d, 3H, J = 6.5 Hz). ESI MS (m/z) 387 $[M + NH_4]^+$.

*5.1.2.36. (R)-4-[4-methoxy-2-(2,2,2-trifluoroacetamido)phenyl]butan-2-yl-methanesulfonate [(R)-**21a**].* This product was obtained starting from (*R*)-**20a** according to the procedure above described. White solid, mp 79–80 °C (diethyl ether-petroleum ether); 84 % yield. ^{1}H NMR and ESI MS data were in agreement with those reported for the racemate (*R*,*S*)-**21a**.

*5.1.2.37. (S)-4-[4-methoxy-2-(2,2,2-trifluoroacetamido)phenyl]butan-2-yl-methanesulfonate [(S)-**21a**].* This product was obtained starting from (*S*)-**20a** according to the procedure above described. White solid, mp 80-1 °C (diethyl ether-petroleum ether); 47 % yield. ^{1}H NMR and ESI MS data were in agreement with those reported for the racemate (*R*,*S*)-**21a**.

*5.1.2.38. (R,S)-7-methoxy-2-methyl-1,2,3,4-tetrahydroquinoline [(R,S)-**22a**].* NaH (60 % in mineral oil, 74 mg, 1.83 mmol) was added under nitrogen at 0 °C to a solution of methanesulfonate (*R*,*S*)-**21a** (460 mg, 1.25 mmol) in dry DMF (5.7 mL). The resulting mixture was stirred at room temperature for 8 h, then it was quenched by adding water and extracted with EtOAc. The organic phases were combined, washed with brine, dried (Na_2SO_4) and concentrated under reduced pressure to give a crude material which was purified by flash chromatography over silica gel (cyclohexane/EtOAc 7:3 as eluent). White solid, 65 % yield. Experimental data were in agreement with those previously reported [47].

*5.1.2.39. (R)-7-methoxy-2-methyl-1,2,3,4-tetrahydroquinoline [(R)-**22a**].* This product was obtained starting from (*S*)-**21a** according to the procedure above described. White solid, mp 86-7 °C (petroleum ether); 90 % yield. ^{1}H NMR and ESI MS data were in agreement with those reported for the racemate (*R*,*S*)-**22a**.

*5.1.2.40. (S)-7-methoxy-2-methyl-1,2,3,4-tetrahydroquinoline [(S)-**22a**].* This product was obtained starting from (*R*)-**21a** according to the procedure above described. White solid, mp 83-4 °C (petroleum ether); 90 % yield. ^{1}H NMR and ESI MS data were in agreement with those reported in literature [48.].

*5.1.2.41. (R,S)-7-methoxy-2-phenyl-1,2,3,4-tetrahydroquinoline [(R,S)-**22b**].* A solution of 7-methoxy-2-phenylquinoline (200 mg, 0.85 mmol) [24] in THF (5 mL) was hydrogenated (5 atm) over Raney Nickel for 6 h at 60 °C. The catalyst was filtered on Celite, the filtrate was concentrated *in vacuo*, and the residue purified by silica gel flash chromatography (cyclohexane/EtOAc 9:1 as eluent). Oil; 67 % yield. ^{1}H NMR (200 MHz, $CDCl_3$) δ: 7.41-7.30 (m, 5H), 6.93 (d, 1H, J = 8.0 Hz), 6.28 (dd, 1H, J = 2.0 and 8.0 Hz), 6.14 (d, 1H, J = 2.0 Hz), 4.44 (dd, 1H, J = 4.0 and 8.0 Hz), 4.13 (brs, 1H), 3.77 (s, 3H), 2.90-2.62 (m, 2H), 2.13-1.98 (m, 2H). ESI MS (m/z) 240 $[M+H]^+$.

*5.1.2.42. (R,S)-2-[7-methoxy-2-methyl-3,4-dihydroquinolin-1(2H)-yl] acetonitrile [(R,S)-**23a**].* Bromoacetonitrile (72 µl, 0.77 mmol) was added to a solution of (*R*,*S*)-**22a** (100 mg, 0.56 mmol) in DMF (1.7 mL). The resulting mixture was stirred at 100 °C under nitrogen atmosphere for 7 h, then it was quenched by adding water and extracted with EtOAc. The organic phases were combined, washed with brine, dried (Na_2SO_4) and concentrated under reduced pressure to give a crude material which

was purified by flash chromatography over silica gel (cyclohexane/EtOAc 9:1 as eluent). Oil; 50 % yield. ^{1}H NMR (200 MHz, $CDCl_3$) δ: 6.96 (d, 1H, J = 8.0 Hz), 6.34 (dd, 1H, J = 2.0 and 8.0 Hz), 6.23 (d, 1H, J = 2.0 Hz), 4.24 (d, 1H, J = 18.0 Hz), 4.11 (d, 1H, J = 18.0 Hz), 3.81 (s, 3H), 3.58-3.50 (m, 1H), 2.79-2.63 (m, 2H), 2.08-1.91 (m, 1H), 1.86-1.72 (m, 1H), 1.28 (d, 3H, J = 6.5 Hz). ESI MS (m/z) 217 $[M+H]^+$.

*5.1.2.43. (R)-2-[7-methoxy-2-methyl-3,4-dihydroquinolin-1(2H)-yl] acetonitrile [(R)-**23a**].* This product was obtained starting from (*R*)-**22a** according to the procedure above described. Oil; 50 % yield. ^{1}H NMR and ESI MS data were in agreement with those reported for the racemate (*R,S*)-**23a**.

*5.1.2.44. (S)-2-[7-methoxy-2-methyl-3,4-dihydroquinolin-1(2H)-yl] acetonitrile [(S)-**23a**].* This product was obtained starting from (*S*)-**22a** according to the procedure above described. Oil; 42 % yield. ^{1}H NMR and ESI MS data were in agreement with those reported for the racemate (*R,S*)-**23a**.

*5.1.2.45. (R,S)-2-[7-methoxy-2-phenyl-3,4-dihydroquinolin-1(2H)-yl] acetonitrile [(R,S)-**23b**].* Bromoacetonitrile (130 μl, 1.9 mmol), a catalytic amount of KI and K_2CO_3 (87 mg, 0.42 mmol) were added to a solution of 7-methoxy-2-phenyl-1,2,3,4-tetrahydroquinoline (*R,S*)-**22b** (100 mg, 0.42 mmol) in dry DMF (1.7 mL) and the resulting mixture was heated at 80 °C under nitrogen atmosphere for 16 h. The reaction mixture was poured into water and then extracted with EtOAc. The organic phases were combined, washed with brine, dried (Na_2SO_4) and concentrated under reduced pressure to give a crude material that was purified by silica gel flash chromatography (cyclohexane/EtOAc 8:2 as eluent). Oil; 58 % yield. ^{1}H NMR (200 MHz, $CDCl_3$) δ: 7.44-7.30 (m, 5H), 7.00 (d, 1H, J = 8.0 Hz), 6.43-6.38 (m, 2H), 4.53-4.48 (m, 1H), 4.19 (d, 1H, J = 18.0 Hz), 3.90 (d, 1H, J = 18.0 Hz), 3.84 (s, 3H), 2.78-2.62 (m, 2H), 2.28-2.01 (m, 2H). ESI MS (m/z) 279 $[M+H]^+$.

*5.1.2.46. (R,S)–N-{2-[7-methoxy-2-methyl-3,4-dihydroquinolin-1(2H)-yl]ethyl}propionamide [(R,S)-**24a**].* This product was obtained starting from nitrile (*R,S*)-**23a** according to the procedure above described. Flash chromatography over silica gel (cyclohexane/EtOAc 4:6 as eluent). White solid, mp 115-6 °C (diethyl ether-petroleum ether); 83 % yield. ^{1}H NMR (400 MHz, CD_3OD) δ: 6.81 (d, 1H, J = 8.0 Hz), 6.30 (d, 1H, J = 2.5 Hz), 6.12 (dd, 1H, J = 2.5 and 8.0 Hz), 3.75 (s, 3H), 3.52 (ddq, 1H, $J_1 \approx J_2$ = 4.5 and 6.5 Hz), 3.47-3.27 (m, 4H), 2.77 (ddd, 1H, J = 5.5, 12.0 and 16.0 Hz), 2.60 (ddd, 1H, $J_1 \approx J_2$ = 4.5 and 16.0 Hz), 2.20 (q, 2H, J = 7.5 Hz), 1.88 (dddd, 1H, $J_1 \approx J_2$ = 4.5 and $J_3 \approx J_4$ = 12.5 Hz), 1.76 (dddd, 1H, $J_1 \approx J_2$ = 4.5, 5.5 and 12.5 Hz), 1.15 (d, 3H, J = 6.5 Hz), 1.13 (t, 3H, J = 7.5 Hz). ^{13}C NMR (100 MHz, CD_3OD) δ: 176.0, 159.3, 144.6, 128.92, 128.90, 114.2, 96.9, 65.6, 54.2, 52.6, 36.7, 28.8, 27.8, 22.6, 17.5, 9.0. ESI MS (m/z) 277 $[M+H]^+$. Analytical HPLC analysis on a Chiralcel (Chiralpak) AD-H column, using hexane/*i*-PrOH 9:1 as eluent, at 308 nm and a flow rate = 1.0 mL/min. Retention time 7.59 and 9.84; ee = 0 %.

*5.1.2.47. (R)-N-{2-[7-methoxy-2-methyl-3,4-dihydroquinolin-1(2H)-yl] ethyl}propionamide [(R)-**24a**].* This product was obtained starting from nitrile (*R*)-**23a** according to the procedure above described. Flash chromatography over silica gel (cyclohexane/EtOAc 4:6 as eluent). White solid, mp 96-7 °C (diethyl ether-petroleum ether); 65 % yield. ^{1}H NMR, ^{13}C NMR and ESI MS data were in agreement to those reported for the racemate (*R,S*)-**24a**. $[\alpha]_D^{20} = +47.23$ (*c* 0.487 in $CHCl_3$). The enantiomeric purity of the product was determined by analytical HPLC analysis on a Chiralcel (Chiralpak) AD-H column, using hexane/*i*-PrOH 9:1 as eluent, at 308 nm and a flow rate = 1.0 mL/min. Retention time 7.80 min, ee > 99 %. HRMS (ESI): m/z calculated for $C_{16}H_{25}N_2O_2$, $[M+H]^+$ 277.1916; found 277.1909.

*5.1.2.48. (S)–N-{2-[7-methoxy-2-methyl-3,4-dihydroquinolin-1(2H)-yl] ethyl}propionamide [(S)-**24a**].* This product was obtained starting from nitrile (*S*)-**23a** according to the procedure above described. Flash chromatography over silica gel (cyclohexane/EtOAc 4:6 as eluent). White solid, mp 95-7 °C (diethyl ether-petroleum ether); 96 % yield. ^{1}H NMR, ^{13}C NMR and ESI MS data were in agreement to those reported for the racemate (*R,S*)-**24a**. $[\alpha]_D^{20} = -47.39$ (*c* 0.517 in $CHCl_3$). The enantiomeric purity of the product was determined by analytical HPLC analysis on a Chiralcel (Chiralpak) AD-H column, using hexane/*i*-PrOH 9:1 as eluent, at 308 nm and a flow rate = 1.0 mL/min. Retention time 10.17 min, ee > 99 %. HRMS (ESI): m/z calculated for $C_{16}H_{25}N_2O_2$, $[M+H]^+$ 277.1916; found 277.1907.

*5.1.2.49. (R,S)–N-{2-[7-methoxy-2-phenyl-3,4-dihydroquinolin-1(2H)-yl]ethyl}propionamide [(R,S)-**24b**].* This product was obtained starting from nitrile (*R,S*)-**23b** according to the procedure above described. Flash chromatography over silica gel (cyclohexane/EtOAc 4:6 as eluent). White solid, mp 110-1 °C (EtOAc-petroleum ether); 85 % yield. ^{1}H NMR (400 MHz, CD_3OD) δ: 7.30-7.12 (m, 5H), 6.79 (d, 1H, J = 8.0 Hz), 6.45 (d, 1H, J = 2.5 Hz), 6.15 (dd, 1H, J = 2.5 and 8.0 Hz), 4.63 (dd, 1H, $J_1 \approx J_2$ = 4.5 Hz), 3.78 (s, 3H), 3.59-3.52 (m, 1H), 3.41-3.29 (m, 2H), 3.14-3.07 (m, 1H), 2.49 (ddd, 1H, $J_1 \approx J_2$ = 4.5 and 15.5 Hz), 2.38 (ddd, 1H, J = 4.5, 12.0 and 15.5 Hz), 2.16-2.07 (m, 2H), 2.18 (q, 2H, J = 7.5 Hz), 1.99 (dddd, 1H, $J_1 \approx J_2 \approx J_3$ 4.5 and 12.5 Hz), 1.07 (t, 3H, J = 7.5 Hz). ^{13}C NMR (50 MHz, $CDCl_3$) δ: 173.9, 159.5, 145.6, 143.7, 129.6, 128.5, 127.1, 126.6, 115.1, 100.7, 97.2, 61.9, 55.3, 49.9, 37.0, 29.6, 29.2, 22.8, 9.7. ESI MS (m/z) 339 $[M+H]^+$. HPLC purity 96.7 % (t_R 4.34).

*5.1.2.50. (R,S)-methyl 2-(trifluoromethylsulfonyloxy)propanoate [(R,S)-**25**].* A solution of methyl-(*R,S*)-lactate (0.38 ml, 3.3 mmol) in dry DCM (9 mL) was cooled to −15 °C and treated with trifluoromethane sulfonic anhydride (0.77 mL, 4.6 mmol) and 2,6-lutidine (0.53 mL, 4.6 mmol) under an N_2 atmosphere. After stirring at room temperature for 16 h, the reaction mixture was concentrated to yield an oil residue that was purified by flash chromatography (cyclohexane/EtOAc 8:2 as eluent). Oil, 70 % yield. Characterization data (^{1}H NMR and ^{13}C NMR) were in agreement with those reported in literature for the (*S*)-enantiomer [25].

*5.1.2.51. (R,S)-methyl 2-[7-methoxy-3,4-dihydroquinolin-1(2H)-yl]propanoate [(R,S)-**26**].* 2,6-Lutidine (333 mg, 3.1 mmol) and (*R,S*)-**25** (700 mg, 3 mmol) were added dropwise under nitrogen to a stirred solution of 7-methoxy-1,2,3,4-tetrahydroquinoline (440 mg, 2.7 mmol) in dry CH_3CN (12 mL). The resulting mixture was stirred 16 h at 70 °C, then quenched by adding water and extracted with EtOAc. The organic phases were combined, washed with brine, dried (Na_2SO_4) and concentrated under reduced pressure to give a crude material which was purified by flash chromatography over silica gel (cyclohexane/EtOAc 9:1 as eluent). Oil; 82 % yield. ^{1}H NMR (200 MHz, $CDCl_3$) δ: 6.89 (d, 1H, J = 8.0 Hz), 6.21-6.17 (m, 2H), 4.49 (q, 1H, J = 7.0 Hz), 3.76 (s, 3H), 3.72 (s, 3H), 3.36-3.26 (m, 2H), 2.76-2.67 (m, 2H), 1.99-1.87 (m, 2H), 1.50 (d, 3H, J = 7.0 Hz). ESI MS (m/z) 250 $[M+H]^+$.

*5.1.2.52. (R)-methyl 2-[7-methoxy-3,4-dihydroquinolin-1(2H)-yl]propanoate [(R)-**26**].* This product was obtained starting from (*S*)-methyl 2-(trifluoromethanesulfonyloxy)propanoate [25] using the procedure above described for (*R,S*)-**26**. Oil; 78 % yield. ^{1}H NMR and ESI MS data were in agreement with those reported for the racemate (*R,S*)-**26**.

*5.1.2.53. (S)-methyl 2-[7-methoxy-3,4-dihydroquinolin-1(2H)-yl]propanoate [(S)-**26**].* This product was obtained starting from (*R*)-methyl 2-(trifluoromethanesulfonyloxy)propanoate [26] using the procedure above described for (*R,S*)-**26**. Oil; 78 % yield. ^{1}H NMR and ESI MS data were in agreement with those reported for the racemate (*R,S*)-**26**.

*5.1.2.54. (R,S)-2-[7-methoxy-3,4-dihydroquinolin-1(2H)-yl]propan-1-ol [(R,S)-**27**].* A solution of (*R,S*)-**26** (200 mg, 0.8 mmol) in dry THF (4 mL) was added dropwise at 0 °C to a suspension of $LiAlH_4$ (31 mg, 0.8 mmol) in dry THF (3 mL) stirred under nitrogen atmosphere. The resulting mixture was stirred at room temperature for 1 h, then it was quenched by adding at 0 °C EtOAc and H_2O, and then filtered on Celite. The filtrate was extracted with EtOAc, the organic phases were combined, washed with brine, dried (Na_2SO_4) and concentrated under reduced pressure to give a crude material which was purified by flash chromatography over silica gel (cyclohexane/EtOAc 7:3 as eluent). Oil; 97 % yield. ^{1}H NMR (200 MHz, $CDCl_3$) δ: 6.91 (d, 1H, J = 8.0 Hz), 6.41 (d, 1H, J = 2.0 Hz), 6.24 (dd, 1H, J = 2.0 and 8.0 Hz), 4.17-4.02 (m, 1H), 3.78 (s, 3H), 3.75-3.61 (m, 2H), 3.20-3.05 (m, 2H), 2.78-2.71 (m, 2H), 1.96-1.87 (m, 2H), 1.12 (d, 3H, J = 6.5 Hz). ESI MS (*m/z*) 222 $[M+H]^+$.

5.1.2.55. (R)-2-[7-methoxy-3,4-dihydroquinolin-1(2H)-yl]propan-1-ol [(R)-27]. This product was obtained starting from (*R*)-**26** and using the procedure above described for (*R,S*)-**27**. Oil; 93 % yield. ^{1}H NMR and ESI MS data were in agreement with those reported for the racemate (*R,S*)-**27**.

5.1.2.56. (S)-2-[7-methoxy-3,4-dihydroquinolin-1(2H)-yl]propan-1-ol [(S)-27]. This product was obtained starting from (*S*)-**26** and using the procedure above described for (*R,S*)-**27**. Oil; 93 % yield. ^{1}H NMR and ESI MS data were in agreement with those reported for the racemate (*R,S*)-**27**.

*5.1.2.57. (R)-2-{2-[7-methoxy-3,4-dihydroquinolin-1(2H)-yl]propyl}-isoindoline-1,3-dione [(R)-**28**].* A solution of DCAD (250 mg, 0.68 mmol) in dry THF (2.7 mL) was added dropwise to a solution of alcohol (*R*)-**27** (100 mg, 0.45 mmol), phthalimide (100 mg, 0.68 mmol) and PPh_3 (178 mg, 0.68 mmol) in dry THF (1.8 mL) stirred under nitrogen. The resulting mixture was stirred at room temperature for 24 h, then the solvent was evaporated under reduced pressure and the residue taken up with DCM. The solid was removed by filtration, the filtrate evaporated under reduced pressure and the residue purified by flash chromatography over silica gel (cyclohexane/EtOAc 9:1 as eluent). Oil; 47 % yield. ^{1}H NMR (200 MHz, $CDCl_3$) δ: 7.81-7.65 (m, 4H), 6.73 (d, 1H, J = 8.0 Hz), 6.40 (d, 1H, J = 2.0 Hz), 6.02 (dd, 1H, J = 2.0 and 8.0 Hz), 4.85-4.59 (m, 1H), 4.03-3.86 (m, 1H), 3.73 (s, 3H), 3.63 (dd, 1H, J = 6.5 and 15.0 Hz), 3.38-3.13 (m, 2H), 2.67-2.60 (m, 2H), 1.93-1.81 (m, 2H), 1.27 (d, 3H, J = 6.5 Hz). ESI MS (*m/z*) 351 $[M+H]^+$.

*5.1.2.58. (S)-2-{2-[7-methoxy-3,4-dihydroquinolin-1(2H)-yl]propyl}-isoindoline-1,3-dione [(S)-**28**].* This product was obtained starting from alcohol (*S*)-**27** according to the procedure above described. Oil; 52 % yield. ^{1}H NMR and ESI MS data were in agreement with those reported for the (*R*)-enantiomer.

*5.1.2.59. (R)-N-{2-[7-methoxy-3,4-dihydroquinolin-1(2H)-yl]propyl} propionamide [(R)-**29**].* Glacial acetic acid (28 mg, 0.46 mmol) and NH_2NH_2 H_2O (45 μl, 0.92 mmol) were added to a solution of (*R*)-**28** (80 mg, 0.23 mmol) in dry CH_3OH (2.6 mL) and the resulting mixture was stirred under reflux for 4 h. The solid was filtered and the filtrate evaporated under reduced pressure to yield a residue which was taken up with EtOAc and extracted twice with 2 N HCl. The aqueous phases were combined, basified with a saturated aqueous solution of $NaHCO_3$ and extracted with EtOAc. The organic phases were combined, washed with brine, dried (Na_2SO_4) and concentrated under reduced pressure to give a crude material which was used without any further purification.

Propionic anhydride (23 μl, 0.2 mmol) was added to a solution of the crude above amine and Et_3N (36 μl, 0.26 mmol) in dry THF (1.2 mL). The resulting mixture was stirred 1 h at room temperature, then the solvent was evaporated under reduced pressure to yield a crude residue which was purified by flash chromatography over silica gel (cyclohexane/EtOAc 6:4 as eluent). Oil; 81 % yield. ^{1}H NMR (400 MHz, $CDCl_3$) δ: 6.89 (d, 1H, J = 8.0 Hz), 6.34 (d, 1H, J = 2.5 Hz), 6.20 (dd, 1H, J = 2.5 and 8.0 Hz), 5.58 (brs, 1H), 4.13-4.05 (m, 1H), 3.77 (s, 3H), 3.57-3.49 (m, 1H), 3.32-3.25 (m, 1H), 3.11-3.05 (m, 2H), 2.78-2.64 (m, 2H), 2.13 (q, 2H, J = 7.5 Hz), 1.93-1.88 (m, 2H), 1.16 (d, 3H, J = 6.5 Hz), 1.09 (t, 3H, J = 7.5 Hz). ^{13}C NMR (50 MHz, $CDCl_3$) δ: 173.8, 159.2, 146.7, 129.9, 116.4, 100.8, 98.1, 55.2, 51.1, 41.7, 40.2, 29.6, 27.5, 22.6, 14.3, 9.8. ESI MS (*m/z*) 277 $[M+H]^+$. The enantiomeric purity of the product was determined by analytical HPLC analysis on a Chiralcel (Chiralpak) OD-H column, using hexane/*i*-PrOH 8:2 as eluent, at 307 nm and a flow rate = 1.0 mL/min. Retention time 9.73, ee = 84 %. $[\alpha]_D^{20}$ = −2.11 (*c* 0.640 in $CHCl_3$).

*5.1.2.60. (S)–N-{2-[7-methoxy-3,4-dihydroquinolin-1(2H)-yl]propyl} propionamide [(S)-**29**].* This product was obtained starting from (*S*)-**28** according to the procedure above described. Oil; 76 % yield. ^{1}H NMR, ^{13}C NMR and ESI MS data were in agreement to those reported for the (*R*)-enantiomer. The enantiomeric purity of the product was determined by analytical HPLC analysis on a Chiralcel (Chiralpak) OD-H column, using hexane/*i*-PrOH 8:2 as eluent, at 307 nm and a flow rate = 1.0 mL/min. Retention time 7.40, ee = 95 %. $[\alpha]_D^{20}$ = + 2.47 (*c* 0.810 in $CHCl_3$).

*5.1.2.61. (R,S)-1-(2-chloropropyl)-7-methoxy-1,2,3,4-tetrahydroquinoline [(R,S)-**30**].* Mesyl chloride (0.155 mL, 2 mmol) was added dropwise under nitrogen to a solution of alcohol (*R,S*)-**27** (220 mg, 1 mmol) and Et_3N (0.66 mL, 4.73 mmol) in dry DCM (4.5 mL). The resulting mixture was stirred 20 h at room temperature, then it was quenched by adding water and extracted with DCM. The organic phases were combined, washed with brine, dried (Na_2SO_4) and concentrated under reduced pressure to give a crude material which was purified by flash chromatography over silica gel (cyclohexane/DCM 7:3 as eluent). Oil; 37 % yield. ^{1}H NMR (200 MHz, $CDCl_3$) δ: 6.90 (d, 1H, J = 8.0 Hz), 6.19 (dd, 1H, J = 2.5 and 8.0 Hz), 6.09 (d, 1H, J = 2.5 Hz), 4.38-4.29 (m, 1H), 3.78 (s, 3H), 3.59-3.30 (m, 4H), 2.75-2.68 (m, 2H), 1.99-1.87 (m, 2H), 1.56 (d, 3H, J = 6.5 Hz). ESI MS (*m/z*) 240 $[M+H]^+$.

*5.1.2.62. (R,S)–N-{1-[7-methoxy-3,4-dihydroquinolin-1(2H)-yl]propan-2-yl}propionamide [(R,S)-**31**].* NaN_3 (87 mg, 1.34 mmol) was added under nitrogen to a solution of (*R,S*)-**30** (130 mg, 0.54 mmol) in dry DMF (1.8 mL). The resulting mixture was stirred at 110 °C for 4 h, then it was quenched by adding water and extracted with EtOAc. The organic phases were combined, washed with brine, dried (Na_2SO_4) and concentrated under reduced pressure to give a crude material which was used without any further purification. ESI MS (*m/z*) 247 $[M+H]^+$.

A solution of the above crude azide in *i*-PrOH (13 mL) and propionic anhydride (0.97 mL, 7.6 mmol) was hydrogenated (4 atm) over Pd/C 10 % (30 mg) for 6 h at room temperature. The catalyst was filtered on Celite, the filtrate was concentrated *in vacuo* to give a crude material which was purified by flash chromatography over silica gel (cyclohexane/EtOAc 1:1 as eluent). White solid, mp 95-6 °C (diethyl ether-petroleum ether); 55 % yield. ^{1}H NMR (200 MHz, $CDCl_3$) δ: 6.84 (d, 1H, J = 8.0 Hz), 6.40 (d, 1H, J = 2.5 Hz), 6.16 (dd, 1H, J = 2.5 and 8.0 Hz), 5.31 (brd, 1H), 4.41-4-27 (m, 1H), 3.80 (s, 3H), 3.51 (dd, 1H, J = 6.0 and 14.5 Hz), 3.40-3.21 (m, 2H), 3.02 (dd, 1H, J = 7.5 and 14.5 Hz), 2.73-2.66 (m, 2H), 2.16 (q, 2H, J = 7.5 Hz), 1.97-1.85 (m, 2H), 1.23 (d, 3H, J = 6.5 Hz), 1.09 (t, 3H, J = 7.5 Hz). ^{13}C NMR (100 MHz, $CDCl_3$) δ: 173.4, 159.3, 146.5, 129.7, 115.0, 100.7, 97.6, 56.4, 55.3, 50.4, 44.1, 29.8, 27.3, 22.3, 18.9, 9.7. ESI MS (*m/z*) 277 $[M+H]^+$. Analytical HPLC analysis on a Chiralcel (Chiralpak) OD-H column, using hexane/*i*-PrOH 9:1 as eluent, at 307 nm and a flow rate = 1.0 mL/min. Retention time 12.59 and 15.12, ee = 0 %.

5.2. Pharmacology

5.2.1. Binding assay

Binding affinities were determined using 2-[^{125}I]iodomelatonin as the labelled ligand in competition experiments on cloned human MT_1 and MT_2 receptors expressed in NIH3T3 rat fibroblast cells. The characterization of NIH3T3-MT1 and -MT_2 cells had been already described in detail [49,50]. Membranes were incubated for 90 min at 37 °C in binding buffer (Tris-HCl, 50 mM, pH 7.4). The final membrane concentration was 5–10 μg of protein per tube. The membrane protein level was determined in accordance with a previously reported method [51]. 2-[^{125}I]Iodomelatonin (100 pM) and different concentrations of melatonin (10^{-10} – 10^{-6} M) or of the new compounds were incubated with the receptor preparation for 90 min at 37 °C. Nonspecific binding was assessed with 10 μM melatonin; IC_{50} values were determined by nonlinear fitting strategies with the program PRISM (GraphPad Software Inc., San Diego, CA). The pK_i values were calculated from the IC_{50} values in accordance with the Cheng-Prusoff equation [34]. The pK_i values are the mean of at least three independent determinations performed in duplicate.

5.2.2. Functional activity assay

To define the functional activity of the new compounds at MT_1 and MT_2 receptor subtypes, [^{35}S]GTPγS binding assays in NIH3T3 cells expressing human-cloned MT_1 or MT_2 receptors were performed. The amount of bound [^{35}S]GTPγS is proportional to the level of the analogue-induced G-protein activation and is related to the intrinsic activity of the compound under study. The detailed description and validation of this method were reported elsewhere [49,52]. Membranes (15–25 μg of protein, final incubation volume 100 μL) were incubated at 30 °C for 30 min in the presence and in the absence of melatonin analogs in an assay buffer consisting of [^{35}S]GTPγS (0.3–0.5 nM), GDP (50 μM), NaCl (100 mM), and $MgCl_2$ (3 mM). Nonspecific binding was defined using [^{35}S]GTPγS (10 μM). In cell lines expressing human MT_1 or MT_2 receptors, melatonin produced a concentration-dependent stimulation of basal [^{35}S]GTPγS binding with a maximal stimulation, above basal levels, of 370 % and 250 % in MT_1 and MT_2 receptors, respectively. Basal stimulation is the amount of [^{35}S]GTPγS specifically bound in the absence of compounds, and it was taken as 100 %. The maximal G-protein activation was measured in each experiment by using melatonin 100 nM. Compounds were added at three different concentrations (one concentration was equivalent to 100 nM melatonin, a second one 10 times smaller, and a third one 10 times larger), and the percent stimulation above basal was determined. The equivalent concentration was estimated on the basis of the ratio of the affinity of the test compound to that of melatonin. It was assumed that at the equivalent concentration the test compound occupies the same number of receptors as 100 nM melatonin. Measurements were performed in triplicate. The relative intrinsic activity (IAr) values were obtained by dividing the maximum ligand-induced stimulation of [^{35}S]GTPγS binding by that of melatonin as measured in the same experiment. By convention, the natural ligand melatonin has an efficacy (E_{max}) of 100 %.

5.2.3. cAMP assays

Chinese Hamster Ovary (CHO) cells stably transfected with human MT_1 or MT_2 receptors were cultured in Ham's F–12K medium supplemented with 10 % fetal bovine serum (FBS), 1 % glutamine, 600 μg/mL geneticin, and 10 μg/mL puromycin. Cells were detached using trypsin after washing with phosphate-buffered saline, followed by centrifugation (10 min at 200×*g*). Cells were then seeded into 96-well white half-area microplate in stimulation buffer composed of Hank Balanced Salt Solution, 5 mM HEPES, 0.5 mM Ro 20–1724, 0.1 % BSA. To assess potency and intrinsic activity, cells were incubated with various concentrations of the tested ligands in the presence of 1 μM forskolin to stimulate cAMP production. The potency of 5-HEAT and **4d** at MT_2 receptors was evaluated as functional antagonists, by testing their ability to restore the forskolin-stimulated cAMP levels reduced by melatonin (1 nM). The cAMP levels were quantified by using the AlphaScreen cAMP Detection Kit (Revvity), following the manufacturer's instructions. The resulting Alpha signal was measured using a Perkin Elmer EnSight Multimode Plate Reader (77).

5.2.4. Cell lines

Human glioma cell lines HOG, U87MG and U87MG-luc (expressing a luciferase reporter gene) were cultured in RPMI 1640 medium (Thermo Fisher Scientific) supplemented with 10 % heat-inactivated fetal bovine serum (Thermo Fisher Scientific), 100 IU/mL penicillin (Thermo Fisher Scientific), and 100 μg/mL streptomycin (Thermo Fisher Scientific). HOG and U87MG were obtained from ATCC, and U87MG-luc was kindly provided by Dr. Andrew L. Kung (Memorial Sloan Kettering Cancer Center, NY, USA).

5.2.5. MTT proliferation assay

Cells (4×10^3 per well) were seeded into 96-well plates, allowed to adhere overnight, and then treated with **4d** (UCM1400) (10^{-9}–10^{-6} M) or the appropriate vehicle for 48 h. After treatment, the culture medium was replaced with an MTT solution (0.5 mg/mL in PBS, Sigma), and cells were incubated for 4 h. The reduced MTT crystals (formazan) were dissolved in a 1:1 isopropanol:DMSO solution for 10 min at room temperature. Absorbance was measured at 570 nm with background subtraction at 690 nm using a SpectraMax 250 spectrophotometer (Molecular Devices).

5.2.6. U87MG orthotopic xenograft model

U87MG-luc cells (5×10^5) suspended in 5 μL of PBS were injected into the right striatum of 8–10-week-old female/male Balb/C nude mice (Charles River International) using a 10-μL Hamilton syringe connected to a Harvard 22 syringe pump (Harvard Apparatus), as previously described [53,54]. Two weeks after tumor implantation, animals were divided into experimental groups: vehicle (0.2 % DMSO, 10^{-4} M 5-HEAT, 10^{-4} M UCM799 or 10^{-4} M **4d** (UCM1400). Treatments were continuously infused (0.25 μL/h) into the right striatum over 14 days using ALZET mini-osmotic pumps (model 1002) and the ALZET brain infusion kit 3 (DURECT Corporation). Before implantation, pumps were pre-filled and primed in sterile 0.9 % saline overnight at 37 °C, following the manufacturer's instructions. Considering the pump infusion rate (0.25 μL/h), the average cerebrospinal fluid volume (35 μL), and production rate (18 μL/h) in mice [55], the expected equilibrium concentration of the compounds in the tumor microenvironment was approximately 10^{-6} M. This concentration corresponds to the effective doses of UCM799, 5-HEAT [15], and **4d** (UCM1400) that showed maximal inhibition in U87MG culture dose–response assays. Fourteen days after treatment, mice were euthanized under deep anesthesia, and the encapsulated tumors were surgically removed. Tumor volume (mm^3) was calculated based on width (a) and length (b) measurements using formula $V = (a^2 \times b)/2$, where $a \leq b$. All procedures followed institutional guidelines for animal welfare and experimental conduct. The study was approved by the Animal Ethics Committee of the A.C. Camargo Cancer Center (ID 076/17) and the Animal Ethics Committee of the Institute of Biosciences, University of São Paulo (ID 284/2017).

5.3. Molecular modelling

5.3.1. Protein preparation

The cryo-electron microscopy (cryo-EM) structures of the activated MT_1 and MT_2 (PDB id 7VGZ, 7VGY and 7VH0 [39]) were used for molecular modelling studies. Hydrogens and capping neutral groups were added and bond orders were assigned with the Protein Preparation

Wizard tool [56] of Maestro [57]. Missing portions of the two receptors, including ICL3 residues (P223-L229 and P236-L242 at the MT_1 and MT_2 receptors, respectively), incomplete side chains and mutated residues ($L108^{ECL1}$, $F129^{3.41}$ and $C140^{3.52}$ of the MT_2 receptor) were restored with Prime [58].

Missing portions of the MT_2 receptor were built by using a chimeric model template designed with Prime [58] through the knowledge-based method, which relies on backbone coordinates (and side chains of conserved residues) from different structures. Specifically, residues at the beginning of TM I (P36–S37) and at the end of TM VIII (L324-N328) were modelled on the thermostabilized construct of the MT_2 receptor in complex with ramelteon (PDB id 6ME9 [37]). A partially unfolded intracytoplasmic region of TM VI (K243–F254) was rebuilt using the cryo-EM structure of the MT_1 receptor in complex with ramelteon (PDB id 7VGZ) [39]. Moreover, in the case of the MT_2 receptor, the disulfide bridge between $C113^{3.25}$ and $C190^{ECL2}$ was rebuilt. Non-conserved residues and missing residues were minimized to refine the model within the Prime procedure. Basic and acidic amino acids were modelled in their charged protonation state, except for histidine residues that were maintained uncharged and $D41/54^{1.46}$ modelled in their neutral state to interact with $V76/89^{2.53}$ backbone carbonyl. The orientation of thiol and hydroxyl groups and of asparagine and glutamine side chains were then adjusted to optimize the hydrogen bonding network. Also, the tautomeric state of histidine residues was selected to maximize the number of H-bond interactions. Hydrogen atoms were minimized with OPLS4 force field [59] by using Impact [60]. A final energy-minimization was conducted with MacroModel [61] applying OPLS4 force field using the Polak-Ribière conjugate gradient method [62] to a convergence threshold of 0.01 kJ mol^{-1} $Å^{-1}$, with fixed backbone atoms.

5.3.2. Protein-ligand docking

Molecular models of MT_1 and MT_2 receptor in complex with **3g**, UCM793, (*R*)-**24a**, (*S*)-**24a**, (*R*)-**29** and (*S*)-**29**, **3a**, and **4d** were generated through a docking procedure based on Glide software [63,64] in standard precision (SP) mode with OPLS4 force field [59]. The structures of ligands were built in Maestro and prepared with the LigPrep tool [57] and energy-minimized using an implicit water model with MacroModel [61]. The docking grids were computed on the prepared receptors and centered on the center of mass of the co-crystallized ligand, selecting inner and outer box dimensions of 10 and 20 Å, respectively. The best ten poses were retrieved and submitted to post-dock minimization. The best pose according to Emodel score, in which the methoxy and amide groups of each ligand established hydrogen bond interactions with $N162/175^{4.60}$ and $Q181/194^{ELC2}$ of MT_1/MT_2 receptors, respectively, was minimized using MacroModel [61] to an energy gradient of 0.05 kJ mol^{-1} $Å^{-2}$. During energy minimization only the ligands and the side chains of the protein within 5 Å of the ligands were free to move.

5.3.3. Molecular dynamics (MD) simulations of *3g*, UCM793, *3a* and *4d* bound to MT_1 and MT_2 receptors

The energy-minimized complexes of the MT_1 and MT_2 receptors bound to **3g**, UCM793, **3a** and **4d** were employed for MD simulations. Each complex was embedded with OPM orientation in a 1-palmitoyl-2-oleyl-*sn*-glycerol-3-phosphocholine (POPC) lipid bilayer and solvated into a TIP3P water box [65] of about 81 × 81 × 120 Å by using the CharmmGUI server [66]. The four systems were imported in *t-leap* for parametrization with Amber20 [67] and were neutralized by adding 11 and 16 chloride ions for the MT_1 and MT_2 receptors, respectively. The ff14sb Amber force field [68] and the general Amber force field (GAFF) [69] were applied to model protein and ligand, respectively. OPLS4 partial atomic charges were assigned to the ligands. Amber Lipid17 parameters for POPC bilayer were assigned to the membrane. Joung-Cheatham parameters were used to model the neutralizing ions [70]. Molecular dynamics (MD) simulations were performed with the *pmemd.cuda* module of Amber20 software [65]. The systems were minimized with *sander* applying three minimization steps of 50,000 cycles, each one passing from steepest descent algorithm to conjugate gradient method after 5000 steps, and with protein backbone fixed with a restraint of 20 kcal mol^{-1} $Å^{-2}$. Membrane was relaxed and the protein-ligand complexes were equilibrated for 4 ns under NVT and for 21 ns under NPT conditions, increasing the temperature up to 298 K and gradually reducing constraints on both the ligand and the protein. Hydrogen atoms were handled with the SHAKE algorithm, and a cutoff of 10 Å was selected to treat the electrostatic and van der Waals interactions. Long-range electrostatic interactions were treated using the Particle Mesh Ewald [71] method. The production phase was carried out for 200 ns (**3g** and UCM793) under NPT conditions with temperature at 298 K controlled by Langevin thermostat [72] with a collision frequency of 2 ps, and pressure was maintained at 1 bar by using the Monte Carlo barostat [73] with a pressure relaxation time of 2 ps.

Molecular dynamics is a useful tool to assess the effect of different ligands on the receptor conformational space [74]. The computational protocol described above was also applied to perform 2 μs-long MD simulations of MT_1 and MT_2 receptors in complex with the subtype selective modulator **4d** in comparison with the MT_1/MT_2 agonist **3a**.

5.3.4. Thermodynamic integration

Alchemical transformation of the tetrahydroquinoline ring of **3g** into the *N*-methylaniline one of UCM793 was performed using the *pmemd.cuda* TI module of Amber20 software [75]. From an MD simulation of **3g** bound to the MT_1 or MT_2 receptor, four snapshots were extracted along 300ns-long MD trajectories. The minimized coordinates of the chosen snapshots were employed to generate dual ligand topologies. For each process, the one-step protocol was adopted, in which non-bonded interactions between unique atoms and the surrounding environment were described by λ-dependent softcore potentials [36]. Parameters α and β modulating the van der Waals and electrostatics softcore functions were set to 0.5 and 12 $Å^2$, respectively. The minimized snapshots were further minimized and equilibrated using $\lambda = 0.5$, as described in Ref. [76]. The SHAKE algorithm was disabled and an integration time-step of 0.001 ps was applied. Then, for each complex, twelve simulations were run at different λ values (0.00922, 0.04794, 0.11505, 0.20634, 0.31608, 0.43738, 0.56262, 0.68392, 0.79366, 0.88495, 0.95206, 0.99078). For each λ-window the systems were submitted to an initial minimization and equilibration protocol up to 298 K in 500 ps in the NPT ensemble with Langevin thermostat [72] and Monte Carlo barostat [73], followed by 5 ns of TI simulations. $\partial V/\partial\lambda$ values were registered after each ps and averaged for each λ-window. Free-energy differences ($\Delta\Delta G_{calc}$) between starting and end points were computed through numerical integration of the averaged $\partial V/\partial\lambda$ values using a twelve-points gaussian quadrature [75]. Similarly to a protocol already applied to aryl-melatonin analogs [77], in the case of the alchemical transformation of the tetrahydroquinoline ring of **3g** into the *N*-methylaniline one of UCM793, $\Delta\Delta G_{calc}$ was obtained by subtracting the free-energy difference due to the alchemical transformation at the MT_1 receptor from the one at the MT_2 receptor.

5.3.5. Molecular dynamics (MD) simulations of (S)-*24a* and (S)-*29* in solution

MD simulations were conducted by solvating the compounds in an orthorhombic box (10 × 10 × 10 Å) containing TIP3P water, chloroform molecules or, in a water solution of ionic strength = 0.15 mol/kg (0.15 M) NaCl. Each system was prepared using Maestro and parametrized with the OPLS4 force field, resulting in simulation boxes containing 1594 TIP3P water molecules, 312 $CHCl_3$ molecules or 1552 TIP3P water molecules and 2 Na^+ and Cl^- ions, respectively. System equilibration was carried out using the default protocol provided by Desmond in the Schrödinger suite. Following equilibration, a 2 μs production run was performed at 300 K under an NVT ensemble, employing a Langevin thermostat with a relaxation time of 1 ps. A total of 40,000 snapshots were collected throughout the simulation, and for (*S*)-**29** (modelled in a

water box or in a 0.15 M NaCl solution) they were projected onto a binned two-dimensional τ_1–τ_2 plot (τ1:C8a-N-Cβ-Cα; τ2:N-Cβ-Cα-Namide). The relative free energy for each bin *i* was computed using the formula:

$$G_i = RT \ln(N_i/N_0)$$

where N_i represents the number of snapshots in bin *i*, and N_0 corresponds to the number in the most populated bin. The convergence was assessed by evaluating the evolution of the free-energy surface during MD simulation.

5.3.6. Principal component analysis (PCA)

Principal component analysis (PCA) was performed on the conformational ensembles obtained from the molecular dynamics simulations of the four protein–ligand complexes: MT_1–**3a**, MT_1–**4d**, MT_2–**3a**, and MT_2–**4d**. For each simulation, the first 500 ns were discarded to exclude the equilibration phase. Frames were then extracted every 2 ns from the last 1.5 μs of production MD (750 total frames for each system). Prior to analysis, each trajectory was aligned to its corresponding reference crystal structure (i.e., 7VGZ and 7VH0 for MT_1 and MT_2, respectively), pre-aligned to one another to ensure that all systems were expressed in a consistent coordinate frame. Structural manipulation and trajectory handling were performed using the *cpptraj* program [78] in Amber20. Only Cα atoms were retained for the PCA. The coordinate matrices from all systems were concatenated to allow direct comparison of the conformational space sampled across complexes. The data were centered and autoscaled (mean = 0; unit variance) to emphasize correlated motions rather than absolute displacements. PCA was performed with software R 4.4.2 [79], using singular value decomposition as implemented in the *prcomp(.)* function. Principal component (PC) score projections were used to describe the distribution of conformations along the first two principal components (PC1 and PC2). Residue-wise contributions to PC1 were quantified from the squared loadings of the Cα atoms, based on a PCA conducted exclusively on frames from MD simulations of the MT_2-**3a** and MT_2-**4d** complexes.

CRediT authorship contribution statement

Annalida Bedini: Writing – review & editing, Writing – original draft, Investigation, Data curation. **Francesca Galvani:** Writing – original draft, Investigation, Data curation. **Gian Marco Elisi:** Writing – review & editing, Visualization, Investigation, Formal analysis. **Laura Scalvini:** Data curation, Investigation, Writing – review & editing. **Michele Mari:** Validation, Investigation, Data curation. **Adriano Recchia:** Validation, Investigation. **Pedro Augusto C.M. Fernandes:** Investigation, Funding acquisition, Formal analysis. **Gabriela S. Kinker:** Visualization, Investigation, Data curation. **Valeria Lucini:** Validation, Investigation, Formal analysis, Data curation. **Francesco Scaglione:** Supervision, Conceptualization. **Fabrizio Vincenzi:** Data curation, Formal analysis, Investigation, Writing – review & editing. **Katia Varani:** Formal analysis, Supervision, Validation, Writing – review & editing. **Regina P. Markus:** Writing – review & editing, Supervision, Methodology, Conceptualization. **Silvia Rivara:** Writing – review & editing, Writing – original draft, Supervision, Project administration, Conceptualization. **Gilberto Spadoni:** Writing – review & editing, Supervision, Methodology, Funding acquisition, Conceptualization. **Marco Mor:** Writing – review & editing, Supervision, Funding acquisition, Conceptualization.

Funding

This work was supported by funding obtained under the National Recovery and Resilience Plan (NRRP), Mission 4 Component 2 Investment 1.3—Call for tender No. 341 of March 15, 2022 of the Italian Ministry of University and Research funded by the European Union#8212; NextGenerationEU, Project code PE0000006, "A multiscale integrated approach to the study of the nervous system in health and disease" (MNESYS).

This work has been funded by the European Union - NextGenerationEU *Mission 4, Component 2, under the Italian Ministry of University and Research (MUR) National Innovation Ecosystem* grant *ECS00000041 - VITALITY* - CUP H33C22000430006.

Financial support provided to PACMF from São Paulo Research Foundation (FAPESP) (2022/09336-0) and the National Council for Scientific and Technological Development (CNPq: 304105/2022-8).

Declaration of competing interest

The authors declare that they have no known competing financial interests or personal relationships that could have appeared to influence the work reported in this paper.

Acknowledgements

This research benefitted from the HPC (High Performance Computing) facility of the University of Parma, Italy (https://www.hpc.unipr.it). We acknowledge ISCRA for awarding this project access to the LEONARDO supercomputer, owned by the EuroHPC Joint Undertaking, hosted by CINECA (Italy), through the following ISCRA C project (GPCRs_TI, id HP10CWKXO9, to G.M.E.). This work has been carried out in the frame of the ALIFAR project, funded by the Italian Ministry of University through the program "Dipartimenti di Eccellenza 2023–2027".

Appendix A. Supplementary data

Supplementary data to this article can be found online at https://doi.org/10.1016/j.ejmech.2025.118445.

Data availability

Data will be made available on request.

References

[1] M.L. Dubocovich, P. Delagrange, D.N. Krause, D. Sugden, D.P. Cardinali, J. Olcese, International union of basic and clinical pharmacology. LXXV. Nomenclature, classification, and pharmacology of G protein-coupled melatonin receptors, Pharmacol. Rev. 62 (3) (2010) 343–380, https://doi.org/10.1124/pr.110.002832.

[2] H.H. Okamoto, E. Cecon, O. Nureki, S. Rivara, R. Jockers, Melatonin receptor structure and signaling, J. Pineal Res. 76 (3) (2024) e12952, https://doi.org/10.1111/jpi.12952.

[3] R. Jockers, P. Delagrange, M.L. Dubocovich, R.P. Markus, N. Renault, G. Tosini, E. Cecon, D.P. Zlotos, Update on melatonin receptors: IUPHAR review 20, Br. J. Pharmacol. 173 (18) (2016) 2702–2725, https://doi.org/10.1111/bph.13536.

[4] A. Oishi, E. Cecon, R. Jockers, Melatonin receptor signaling: impact of receptor oligomerization on receptor function, Int Rev Cell Mol Biol 338 (2018) 59–77, https://doi.org/10.1016/bs.ircmb.2018.02.002.

[5] E. Cecon, A. Oishi, R. Jockers, Melatonin receptors: molecular pharmacology and signalling in the context of system bias, Br. J. Pharmacol. 175 (16) (2018) 3263–3280, https://doi.org/10.1111/bph.13950.

[6] J. Liu, S.J. Clough, A.J. Hutchinson, E.B. Adamah-Biassi, M. Popovska-Gorevski, M. L. Dubocovich, MT1 and MT2 melatonin receptors: a therapeutic perspective, Annu. Rev. Pharmacol. Toxicol. 56 (2016) 361–383, https://doi.org/10.1146/annurev-pharmtox-010814-124742.

[7] D.P. Zlotos, R. Jockers, E. Cecon, S. Rivara, P.A. Witt-Enderby, MT1 and MT2 melatonin receptors: ligands, models, oligomers, and therapeutic potential, J. Med. Chem. 57 (8) (2014) 3161–3185, https://doi.org/10.1021/jm401343c.

[8] J.A. Boutin, P.A. Witt-Enderby, C. Sotriffer, D.P. Zlotos, Melatonin receptor ligands: a pharmaco-chemical perspective, J. Pineal Res. 69 (3) (2020) e12672, https://doi.org/10.1111/jpi.12672.

[9] A. Bedini, J.A. Boutin, C. Legros, D.P. Zlotos, G. Spadoni, Industrial and academic approaches to the search for alternative melatonin receptor ligands: an historical survey, J. Pineal Res. 76 (4) (2024) e12953, https://doi.org/10.1111/jpi.12953.

[10] P. Klosen, S. Lapmanee, C. Schuster, B. Guardiola, D. Hicks, P. Pevet, M.P. Felder-Schmittbuhl, MT1 and MT2 melatonin receptors are expressed in nonoverlapping neuronal populations, J. Pineal Res. 67 (1) (2019) e12575, https://doi.org/10.1111/jpi.12575.

[11] G. Gobbi, S. Comai, Differential function of melatonin MT1 and MT2 receptors in REM and NREM sleep, Front. Endocrinol. 10 (2019) 87, https://doi.org/10.3389/fendo.2019.00087.

[12] M. López-Canul, S.H. Min, L. Posa, D. De Gregorio, A. Bedini, G. Spadoni, G. Gobbi, S. Comai, Melatonin MT1 and MT2 receptors exhibit distinct effects in the modulation of body temperature across the light/dark cycle, Int. J. Mol. Sci. 20 (10) (2019) 2452, https://doi.org/10.3390/ijms20102452.

[13] S. Doolen, D.N. Krause, M.L. Dubocovich, S.P. Duckles, Melatonin mediates two distinct responses in vascular smooth muscle, Eur. J. Pharmacol. 345 (1) (1998) 67–69, https://doi.org/10.1016/s0014-2999(98)00064-8.

[14] R. Ochoa-Sanchez, S. Comai, B. Lacoste, F.R. Bambico, S. Dominguez-Lopez, G. Spadoni, S. Rivara, A. Bedini, D. Angeloni, F. Fraschini, M. Mor, G. Tarzia, L. Descarries, G. Gobbi, Promotion of non-rapid eye movement sleep and activation of reticular thalamic neurons by a novel MT2 melatonin receptor ligand, J. Neurosci. 31 (50) (2011) 18439–18452, https://doi.org/10.1523/JNEUROSCI.2676-11.2011.

[15] G.S. Kinker, L.H. Ostrowski, P.A.C. Ribeiro, R. Chanoch, S.M. Muxel, I. Tirosh, G. Spadoni, S. Rivara, V.R. Martins, T.G. Santos, R.P. Markus, P.A.C.M. Fernandes, MT1 and MT2 melatonin receptors play opposite roles in brain cancer progression, J. Mol. Med. (Berl.) 99 (2) (2021) 289–301, https://doi.org/10.1007/s00109-020-02023-5.

[16] S. Rivara, A. Lodola, M. Mor, A. Bedini, G. Spadoni, V. Lucini, M. Pannacci, F. Fraschini, F. Scaglione, R.O. Sanchez, G. Gobbi, G. Tarzia, N-(substituted-anilinoethyl)amides: design, synthesis, and pharmacological characterization of a new class of melatonin receptor ligands, J. Med. Chem. 50 (26) (2007) 6618–6626, https://doi.org/10.1021/jm700957j.

[17] F. Ferlenghi, M. Mari, G. Gobbi, G.M. Elisi, M. Mor, S. Rivara, F. Vacondio, S. Bartolucci, A. Bedini, F. Fanini, G. Spadoni, N-(Anilinoethyl)amide melatonergic ligands with improved water solubility and metabolic stability, ChemMedChem 16 (19) (2021) 3071–3082, https://doi.org/10.1002/cmdc.202100405.

[18] S. Rivara, F. Vacondio, A. Fioni, C. Silva, C. Carmi, M. Mor, V. Lucini, M. Pannacci, A. Caronno, F. Scaglione, G. Gobbi, G. Spadoni, A. Bedini, P. Orlando, S. Lucarini, G. Tarzia, N-(Anilinoethyl)amides: design and synthesis of metabolically stable, selective melatonin receptor ligands, ChemMedChem 4 (10) (2009) 1746–1755, https://doi.org/10.1002/cmdc.200900240.

[19] G. Spadoni, A. Bedini, S. Lucarini, M. Mari, D.H. Caignard, J.A. Boutin, P. Delagrange, V. Lucini, F. Scaglione, A. Lodola, F. Zanardi, D. Pala, M. Mor, S. Rivara, Highly potent and selective MT2 melatonin receptor full agonists from conformational analysis of 1-Benzyl-2-acylaminomethyl-tetrahydroquinolines, J. Med. Chem. 58 (18) (2015) 7512–7525, https://doi.org/10.1021/acs.jmedchem.5b01066.

[20] S. Rivara, L. Scalvini, A. Lodola, M. Mor, D.H. Caignard, P. Delagrange, S. Collina, V. Lucini, F. Scaglione, L. Furiassi, M. Mari, S. Lucarini, A. Bedini, G. Spadoni, Tetrahydroquinoline ring as a versatile bioisostere of tetralin for melatonin receptor ligands, J. Med. Chem. 61 (8) (2018) 3726–3737, https://doi.org/10.1021/acs.jmedchem.8b00359.

[21] G. Spadoni, A. Bedini, L. Furiassi, M. Mari, M. Mor, L. Scalvini, A. Lodola, A. Ghidini, V. Lucini, S. Dugnani, F. Scaglione, D. Piomelli, K.M. Jung, C. T. Supuran, L. Lucarini, M. Durante, S. Sgambellone, E. Masini, S. Rivara, Identification of bivalent ligands with melatonin receptor agonist and fatty acid amide hydrolase (FAAH) inhibitory activity that exhibit ocular hypotensive effect in the rabbit, J. Med. Chem. 61 (17) (2018) 7902–7916, https://doi.org/10.1021/acs.jmedchem.8b00893.

[22] M. Righi, A. Bedini, G. Piersanti, F. Romagnoli, G. Spadoni, Direct, one-pot reductive alkylation of anilines with functionalized acetals mediated by triethylsilane and TFA. Straightforward route for unsymmetrically substituted ethylenediamine, J. Org. Chem. 76 (2) (2011) 704–707, https://doi.org/10.1021/jo102109f.

[23] Z. Shen, S. Zhang, H. Geng, J. Wang, X. Zhang, A. Zhou, C. Yao, X. Chen, W. Wang, Trideuteromethylation enabled by a sulfoxonium metathesis reaction, Org. Lett. 21 (2) (2019) 448–452, https://doi.org/10.1021/acs.orglett.8b03641.

[24] J. Baek, T. Si, H.Y. Kim, K. Oh, Bioinspired *o*-naphthoquinone-catalyzed aerobic oxidation of alcohols to aldehydes and ketones, Org. Lett. 24 (27) (2022) 4982–4986, https://doi.org/10.1021/acs.orglett.2c02037.

[25] A.K. Chattopadhyay, V.L. Ly, S. Jakkepally, G. Berger, S. Hanessian, Total synthesis of isodaphlongamine H: a possible biogenetic conundrum, Angew Chem. Int. Ed. Engl. 55 (7) (2016) 2577–2581, https://doi.org/10.1002/anie.201510861.

[26] R.J. Lukas, A.Z. Muresan, M.I. Damaj, B.E. Blough, X. Huang, H.A. Navarro, S. W. Mascarella, J.B. Eaton, S.K. Marxer-Miller, F.I. Carroll, Synthesis and characterization of in vitro and in vivo profiles of hydroxybupropion analogues: aids to smoking cessation, J. Med. Chem. 53 (12) (2010) 4731–4748, https://doi.org/10.1021/jm1003232.

[27] M. D'hooghe, S. Catak, S. Stanković, M. Waroquier, Y. Kim, H.-J. Ha, V. Van Speybroeck, N. De Kimpe, Systematic study of halide-induced ring opening of 2-substituted aziridinium salts and theoretical rationalization of the reaction pathways, Eur. J. Org. Chem. (2010) 4920–4931, https://doi.org/10.1002/ejoc.201000486.

[28] G.M. Elisi, A. Bedini, L. Scalvini, C. Carmi, S. Bartolucci, V. Lucini, F. Scaglione, M. Mor, S. Rivara, G. Spadoni, Chiral recognition of flexible melatonin receptor ligands induced by conformational equilibria, Molecules 25 (18) (2020) 4057, https://doi.org/10.3390/molecules25184057.

[29] L.Q. Sun, J. Chen, M. Bruce, J.A. Deskus, J.R. Epperson, K. Takaki, G. Johnson, L. Iben, C.D. Mahle, E. Ryan, C. Xu, Synthesis and structure-activity relationship of novel benzoxazole derivatives as melatonin receptor agonists, Bioorg. Med. Chem. Lett 14 (14) (2004) 3799–3802, https://doi.org/10.1016/j.bmcl.2004.04.082.

[30] C. Mésangeau, B. Pérès, C. Descamps-François, P. Chavatte, V. Audinot, S. Coumailleau, J.A. Boutin, P. Delagrange, C. Bennejean, P. Renard, D. H. Caignard, P. Berthelot, S. Yous, Design, synthesis and pharmacological evaluation of novel naphthalenic derivatives as selective MT(1) melatoninergic ligands, Bioorg. Med. Chem. 18 (10) (2010) 3426–3436, https://doi.org/10.1016/j.bmc.2010.04.008.

[31] S. Rivara, D. Pala, A. Lodola, M. Mor, V. Lucini, S. Dugnani, F. Scaglione, A. Bedini, S. Lucarini, G. Tarzia, G. Spadoni, MT1-selective melatonin receptor ligands: synthesis, pharmacological evaluation, and molecular dynamics investigation of N-{[(3-O-substituted)anilino]alkyl}amides, ChemMedChem 7 (11) (2012) 1954–1964, https://doi.org/10.1002/cmdc.201200303.

[32] S. Rivara, S. Lorenzi, M. Mor, P.V. Plazzi, G. Spadoni, A. Bedini, G. Tarzia, Analysis of structure-activity relationships for MT2 selective antagonists by melatonin MT1 and MT2 receptor models, J. Med. Chem. 48 (12) (2005) 4049–4060, https://doi.org/10.1021/jm048956y.

[33] S. Durieux, A. Chanu, C. Bochu, V. Audinot, S. Coumailleau, J.A. Boutin, P. Delagrange, D.H. Caignard, C. Bennejean, P. Renard, D. Lesieur, P. Berthelot, S. Yous, Design and synthesis of 3-phenyltetrahydronaphthalenic derivatives as new selective MT2 melatoninergic ligands. Part II, Bioorg. Med. Chem. 17 (8) (2009) 2963–2974, https://doi.org/10.1016/j.bmc.2009.03.023.

[34] Y. Cheng, W.H. Prusoff, Relationship between the inhibition constant (Ki) and the concentration of inhibitor which causes 50 per cent inhibition (I50) of an enzymatic reaction, Biochem. Pharmacol. 22 (23) (1973) 3099–3108, https://doi.org/10.1016/0006-2952(73)90196-2.

[35] H. Liu, A.E. Mark, W.F. van Gunsteren, Estimating the relative free energy of different molecular states with respect to a single reference state, J. Phys. Chem. 100 (1996) 9485–9494.

[36] T. Steinbrecher, D.L. Mobley, D.A. Case, Nonlinear scaling schemes for Lennard-Jones interactions in free energy calculations, J. Chem. Phys. 127 (21) (2007) 214108, https://doi.org/10.1063/1.2799191.

[37] L.C. Johansson, B. Stauch, J.D. McCorvy, G.W. Han, N. Patel, X.P. Huang, A. Batyuk, C. Gati, S.T. Slocum, C. Li, J.M. Grandner, S. Hao, R.H.J. Olsen, A. R. Tribo, S. Zaare, L. Zhu, N.A. Zatsepin, U. Weierstall, S. Yous, R.C. Stevens, W. Liu, B.L. Roth, V. Katritch, V. Cherezov, XFEL structures of the human MT2 melatonin receptor reveal the basis of subtype selectivity, Nature 569 (7755) (2019) 289–292, https://doi.org/10.1038/s41586-019-1144-0.

[38] E. Lipka-Belloli, A. Guelzim, S. Yous, J. Lefebvre, C. Descamps-Francois, F. Capet, C. Vaccher, Melatonin receptor agents: synthesis, resolution by HPLC on polysaccharides chiral stationary phases, absolute configuration, and pharmacology of the enantiomers of (+/-)-N-[[2[(7-fluoro-1,2,3,4-tetrahydronaphthalen-1-yl)ethyl]acetamide, Chirality 13 (4) (2001) 199–206, https://doi.org/10.1002/chir.1020.

[39] Q. Wang, Q. Lu, Q. Guo, M. Teng, Q. Gong, X. Li, Y. Du, Z. Liu, Y. Tao, Structural basis of the ligand binding and signaling mechanism of melatonin receptors, Nat. Commun. 13 (1) (2022) 454, https://doi.org/10.1038/s41467-022-28111-3.

[40] John E. Hall, Michael E. Hall, Guyton and Hall Textbook of Medical Physiology, Elsevier, 2020, 14th Edition - June 15.

[41] R. Nonno, V. Lucini, G. Spadoni, M. Pannacci, A. Croce, D. Esposti, C. Balsamini, G. Tarzia, F. Fraschini, B.M. Stankov, A new melatonin receptor ligand with mt1-agonist and MT2-antagonist properties, J. Pineal Res. 29 (4) (2000) 234–240, https://doi.org/10.1034/j.1600-0633.2002.290406.x.

[42] G. Spadoni, A. Bedini, T. Guidi, G. Tarzia, V. Lucini, M. Pannacci, F. Fraschini, Towards the development of mixed MT(1)-agonist/MT(2)-antagonist melatonin receptor ligands, ChemMedChem 1 (10) (2006) 1099–1105, https://doi.org/10.1002/cmdc.200600133.

[43] M. Ettaoussi, A. Sabaouni, M. Rami, J.A. Boutin, P. Delagrange, P. Renard, M. Spedding, D.H. Caignard, P. Berthelot, S. Yous, Design, synthesis and pharmacological evaluation of new series of naphthalenic analogues as melatoninergic (MT1/MT2) and serotoninergic 5-HT2C dual ligands (I), Eur. J. Med. Chem. 49 (2012) 310–323, https://doi.org/10.1016/j.ejmech.2012.01.027.

[44] M. Ettaoussi, A. Sabaouni, B. Pérès, E. Landagaray, O. Nosjean, J.A. Boutin, D. H. Caignard, P. Delagrange, P. Berthelot, S. Yous, Synthesis and pharmacological evaluation of a series of the agomelatine analogues as melatonin MT1/MT2 agonist and 5-HT2C antagonist, ChemMedChem 8 (11) (2013) 1830–1845, https://doi.org/10.1002/cmdc.201300294.

[45] A. Amadei, A.B.M. Linssen, H.J.C. Berendesen, Essential dynamics of proteins, Proteins 17 (1993) 412–425, https://doi.org/10.1002/prot.340170408.

[46] G.M. Elisi, L. Scalvini, A. Lodola, A. Bedini, G. Spadoni, S. Rivara, In silico drug discovery of melatonin receptor ligands with therapeutic potential, Expet Opin. Drug Discov. 17 (2022) 343–354.

[47] M. Kawase, Y. Kikugawa, Intramolecular cyclization of alkylhydroxylamines in acids, Chem. Pharm. Bull. 29 (1980) 1615–1623.

[48] T. Yang, Q. Yin, G. Gu, X. Zhang, A one-pot process for the enantioselective synthesis of tetrahydroquinolines and tetrahydroisoquinolines via asymmetric reductive amination (ARA), Chem. Commun. 54 (52) (2018) 7247–7250, https://doi.org/10.1039/c8cc03586e.

[49] R. Nonno, V. Lucini, M. Pannacci, C. Mazzucchelli, D. Angeloni, F. Fraschini, B. M. Stankov, Pharmacological characterization of the human melatonin Mel1a receptor following stable transfection into NIH3T3 cells, Br. J. Pharmacol. 124 (3) (1998) 485–492, https://doi.org/10.1038/sj.bjp.0701860.

[50] R. Nonno, M. Pannacci, V. Lucini, D. Angeloni, F. Fraschini, B.M. Stankov, Ligand efficacy and potency at recombinant human MT2 melatonin receptors: evidence for agonist activity of some mt1-antagonists, Br. J. Pharmacol. 127 (5) (1999) 1288–1294, https://doi.org/10.1038/sj.bjp.0702658.

[51] M.M. Bradford, A rapid and sensitive method for the quantitation of microgram quantities of protein utilizing the principle of protein-dye binding, Anal. Biochem. 72 (1976) 248–254, https://doi.org/10.1016/0003-2697(76)90527-3.
[52] G. Spadoni, C. Balsamini, A. Bedini, G. Diamantini, B. Di Giacomo, A. Tontini, G. Tarzia, M. Mor, P.V. Plazzi, S. Rivara, R. Nonno, M. Pannacci, V. Lucini, F. Fraschini, B.M. Stankov, 2-[N-Acylamino(C1-C3)alkyl]indoles as MT1 melatonin receptor partial agonists, antagonists, and putative inverse agonists, J. Med. Chem. 41 (19) (1998) 3624–3634, https://doi.org/10.1021/jm970721h.
[53] A.P. Wasilewska-Sampaio, T.G. Santos, M.H. Lopes, M. Cammarota, V.R. Martins, The growth of glioblastoma orthotopic xenografts in nude mice is directly correlated with impaired object recognition memory, Physiol. Behav. 123 (2014) 55–61, https://doi.org/10.1016/j.physbeh.2013.09.012.
[54] M.H. Lopes, T.G. Santos, B.R. Rodrigues, N. Queiroz-Hazarbassanov, I.W. Cunha, A.P. Wasilewska-Sampaio, B. Costa-Silva, F.A. Marchi, L.F. Bleggi-Torres, P. I. Sanematsu, S.H. Suzuki, S.M. Oba-Shinjo, S.K.N. Marie, E. Toulmin, A.F. Hill, V. R. Martins, Disruption of prion protein–HOP engagement impairs glioblastoma growth and cognitive decline and improves overall survival, Oncogene 34 (25) (2015) 3305–3314, https://doi.org/10.1038/onc.2014.261.
[55] C. Marianecci, F. Rinaldi, P.N. Hanieh, L. Di Marzio, D. Paolino, M. Carafa, Drug delivery in overcoming the blood-brain barrier: role of nasal mucosal grafting, Drug Des. Dev. Ther. 11 (2017) 325–335, https://doi.org/10.2147/DDDT.S100075.
[56] G.M. Sastry, M. Adzhigirey, T. Day, R. Annabhimoju, W. Sherman, Protein and ligand preparation: parameters, protocols, and influence on virtual screening enrichments, J. Comput. Aided Mol. Des. 27 (3) (2013) 221–234, https://doi.org/10.1007/s10822-013-9644-8.
[57] Schrödinger Release 2022-2, LigPrep, Schrödinger, LLC, New York, NY, 2022.
[58] Schrodinger Release 2022-2: Prime, Schrödinger, LLC, New York, NY, USA, 2022.
[59] C. Lu, C. Wu, D. Ghoreishi, W. Chen, L. Wang, W. Damm, G.A. Ross, M.K. Dahlgren, E. Russell, C.D. Von Bargen, R. Abel, R.A. Friesner, E.D. Harder, OPLS4: improving force field accuracy on challenging regimes of chemical space, J. Chem. Theor. Comput. 17 (7) (2021) 4291–4300, https://doi.org/10.1021/acs.jctc.1c00302.
[60] Schrödinger Release 2022-2: Impact 9.1, Schrödinger, LLC, New York, NY, 2022.
[61] Schrödinger Release 2022-2: Macromodel 13.2, Schrödinger, LLC, New York, NY, 2022.
[62] E. Polak, G. Ribière, Note sur la convergence de méthodes de directions conjuguées, Revue Française Inf. Rech. Opér. Sér. Rouge. 3 (16) (1969) 35–43, https://doi.org/10.1051/m2an/196903R100351.
[63] Schrödinger Release 2022-2: Glide 9.1, Schrödinger, LLC, New York, NY, 2022.
[64] R.A. Friesner, J.L. Banks, R.B. Murphy, T.A. Halgren, J.J. Klicic, D.T. Mainz, M. P. Repasky, E.H. Knoll, M. Shelley, J.K. Perry, D.E. Shaw, P. Francis, P.S. Shenkin, Glide: a new approach for rapid, accurate docking and scoring. 1. Method and assessment of docking accuracy, J. Med. Chem. 47 (7) (2004) 1739–1749, https://doi.org/10.1021/jm0306430.
[65] W.L. Jorgensen, J. Chandrasekhar, J.D. Madura, Comparison of simple potential functions for simulating liquid water, J. Chem. Phys. 79 (1983) 926–935, https://doi.org/10.1063/1.445869.
[66] E.L. Wu, X. Cheng, S. Jo, H. Rui, K.C. Song, E.M. Dávila-Contreras, Y. Qi, J. Lee, V. Monje-Galvan, R.M. Venable, J.B. Klauda, W. Im, CHARMM-GUI membrane builder toward realistic biological membrane simulations, J. Comput. Chem. 35 (27) (2014) 1997–2004, https://doi.org/10.1002/jcc.23702.
[67] D.A. Case, K. Belfon, I.Y. Ben-Shalom, S.R. Brozell, D.S. Cerutti, T.E. Cheatham, V. W.D. Cruzeiro, T.A. Darden, R.E. Duke, G. Giambasu, M.K. Gilson, H. Gohlke, A. W. Goetz, R. Harris, S. Izadi, S.A. Izmailov, C. Jin, K. Kasavajhala, M.C. Kaymak, E. King, A. Kovalenko, T. Kurtzman, T.S. Lee, S. LeGrand, P. Li, C. Lin, J. Liu, T. Luchko, R. Luo, M. Machado, V. Man, Y. Man, K.M. Merz, Y. Miao, O. Mikhailovskii, G. Monard, H. Nguyen, K.A. O'Hearn, A. Onufriev, F. Pan, S. Pantano, R. Qi, A. Rahnamoun, D.R. Roe, A. Roitberg, C. Sagui, S. Schott-Verdugo, J. Shen, C.L. Simmerling, N.R. Skrynnikov, J. Smith, J. Swails, R. C. Walker, J. Wang, H. Wei, R.M. Wolf, X. Wu, Y. Xue, D.M. York, S. Zhao, P. A. Kollman, Amber 2020, University of California, San Francisco (CA), 2020.
[68] J.A. Maier, C. Martinez, K. Kasavajhala, L. Wickstrom, K.E. Hauser, C. Simmerling, ff14SB: improving the accuracy of protein side chain and backbone parameters from ff99SB, J. Chem. Theor. Comput. 11 (8) (2015) 3696–3713, https://doi.org/10.1021/acs.jctc.5b00255.
[69] J. Wang, R.M. Wolf, J.W. Caldwell, P.A. Kollman, D.A. Case, Development and testing of a general amber force field, J. Comput. Chem. 25 (9) (2004) 1157–1174, https://doi.org/10.1002/jcc.20035. Erratum in: J Comput Chem. 2005;26(1):114.
[70] I.S. Joung, T.E. Cheatham 3rd, Determination of alkali and halide monovalent ion parameters for use in explicitly solvated biomolecular simulations, J. Phys. Chem. B 112 (30) (2008) 9020–9041, https://doi.org/10.1021/jp8001614.
[71] U. Essmann, L. Perera, M.L. Berkowitz, T. Darden, H. Lee, L.G. Pedersen, A smooth particle mesh Ewald method, J. Chem. Phys. 103 (1995) 8577–8593, https://doi.org/10.1063/1.470117.
[72] R.J. Loncharich, B.R. Brooks, R.W. Pastor, Langevin dynamics of peptides: the frictional dependence of isomerization rates of N-acetylalanyl-N'-methylamide, Biopolymers 32 (5) (1992) 523–535, https://doi.org/10.1002/bip.360320508.
[73] R. Faller, J.J. de Pablo, Constant pressure hybrid molecular dynamics-Monte Carlo simulations, J. Chem. Phys. 116 (2002) 55–59, https://doi.org/10.1063/1.1420460.
[74] G.M. Elisi, G. Bottegoni, Impact of G protein-coupled receptor conformation on signaling bias: integrating simulations and biophysical experiments, Pharmacol. Ther. 274 (2025) 108905.
[75] L.F. Song, T.S. Lee, C. Zhu, D.M. York, K.M. Merz Jr., Using AMBER18 for relative free energy calculations, J. Chem. Inf. Model. 59 (7) (2019) 3128–3135, https://doi.org/10.1021/acs.jcim.9b00105.
[76] J.W. Kaus, L.T. Pierce, R.C. Walker, J.A. McCammont, Improving the efficiency of free energy calculations in the amber molecular dynamics package, J. Chem. Theor. Comput. 9 (9) (2013), https://doi.org/10.1021/ct400340s.
[77] M. Mari, G.M. Elisi, A. Bedini, S. Lucarini, M. Retini, V. Lucini, F. Scaglione, F. Vincenzi, K. Varani, R. Castelli, M. Mor, S. Rivara, G. Spadoni, 2-Arylmelatonin analogues: probing the 2-phenyl binding pocket of melatonin MT_1 and MT_2 receptors, Eur. J. Med. Chem. 243 (2022) 114762, https://doi.org/10.1016/j.ejmech.2022.114762.
[78] D.R. Roe, T.R. Cheatham III, PTRAJ and CPPTRAJ: software for processing and analysis of molecular dynamics trajectory data, J. Chem. Theoy Comput 9 (2013) 3084–3095, https://doi.org/10.1021/ct400341p.
[79] R Core Team, _R: a Language and Environment for Statistical Computing_, R Foundation for Statistical Computing, Vienna, Austria, 2024. https://www.R-project.org/.